



European Research Council
Established by the European Commission

Pier Monni (CERN)
[pier.monni@cern.ch]

Precision Higgs Physics, QCD & Parton Showers [1/3]

PSI summer school - Zuoz, Aug 2024



CERN

Tentative outline of the lectures

- Lecture 1 (Monday): Collider physics & strong interactions
 - Introduction to LHC Physics & the Higgs sector
 - Exploring the Higgs boson with Quantum Chromodynamics (QCD)
- Lecture 2 (Thursday): Radiative corr^{ns} & Collider observables
 - Infrared & Collinear (IRC) safety and differential distributions
 - QCD beyond the standard perturbation theory
- Lecture 3 (Friday): Introduction to Parton Showers & Jets
 - Building a toy parton shower for Higgs production in gluon fusion
 - Modern event generators and hadronic jets

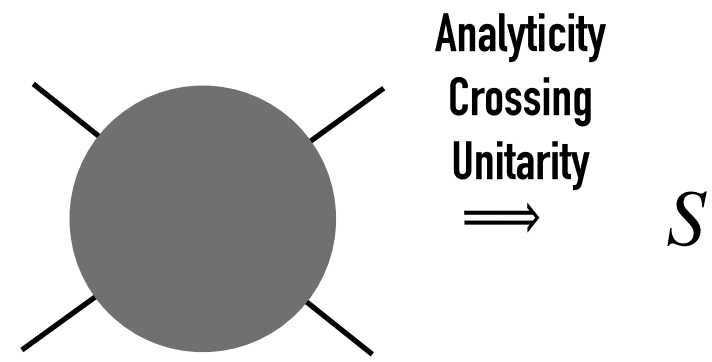
Disclaimer

Not enough time to cover in detail all the aspects that we'll touch upon. Please ask me for extra references if you are interested in reading more about a topic

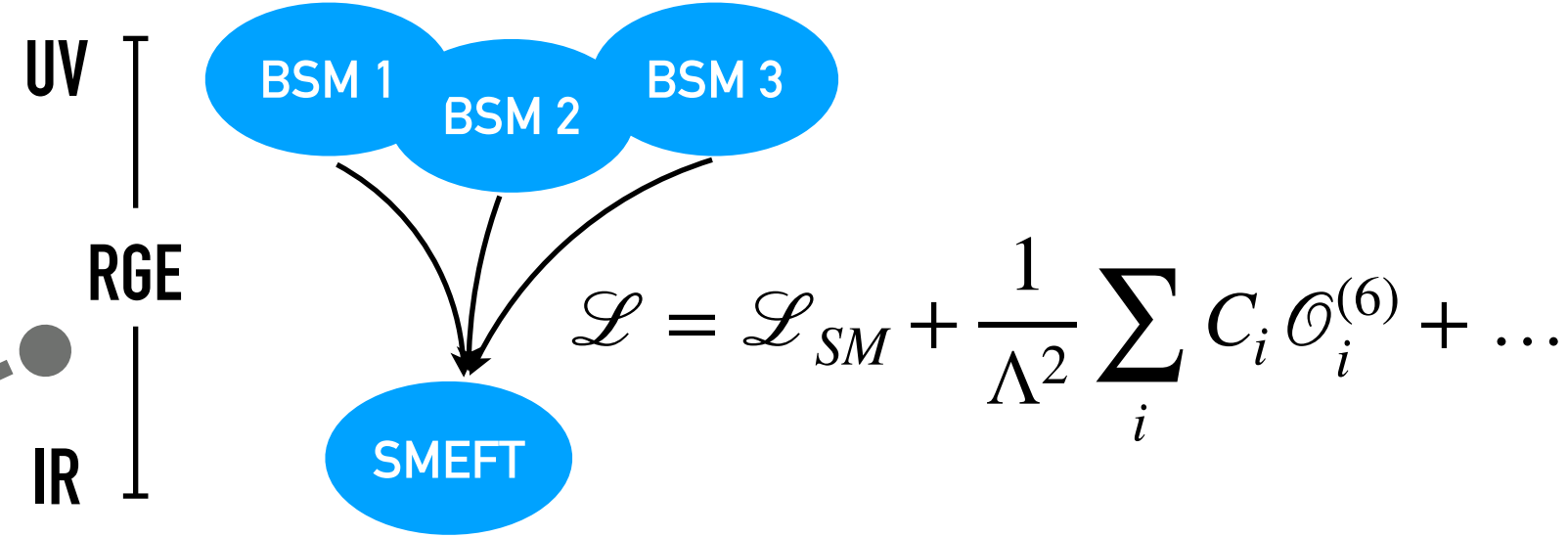
Collider Physics & Strong interactions

The incredibly diverse collider physics landscape

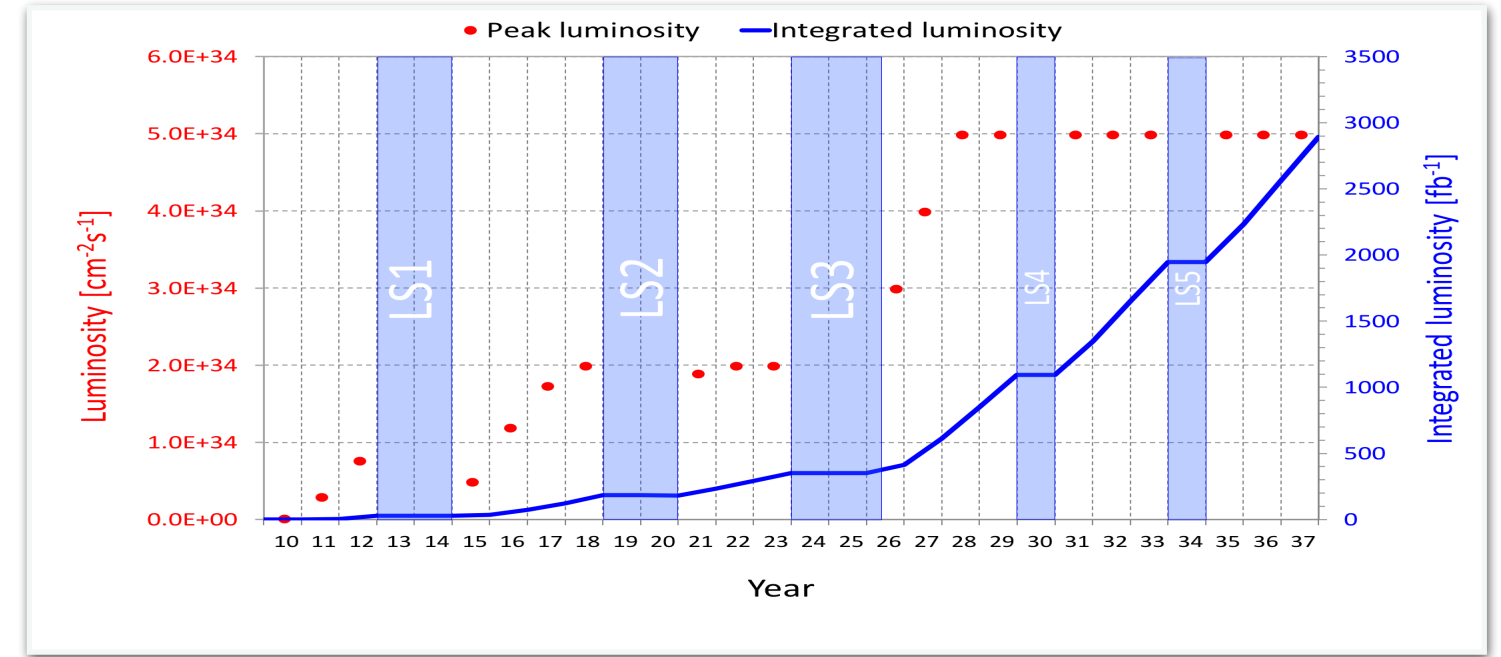
Formal developments



EFTs & New Physics models

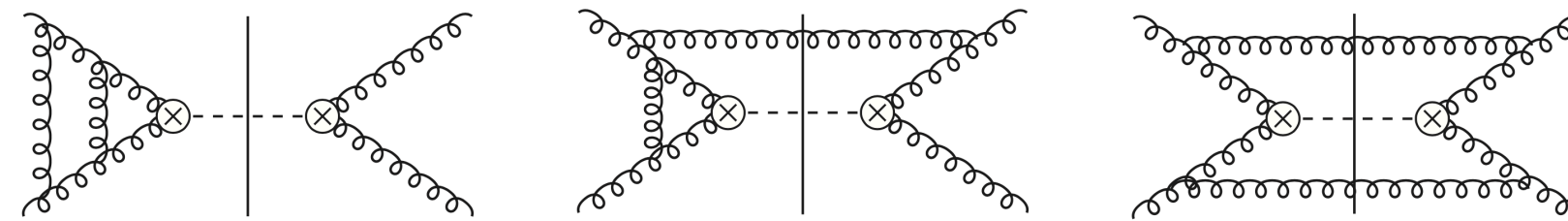


Swathes of experimental results



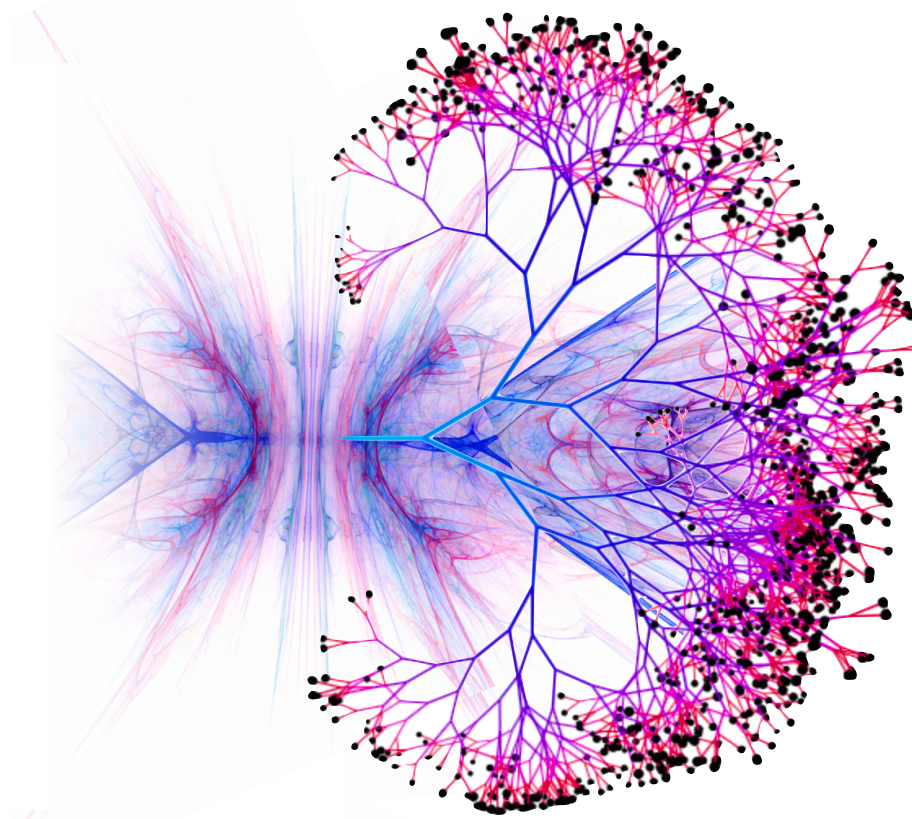
Theory
developments

Perturbative methods

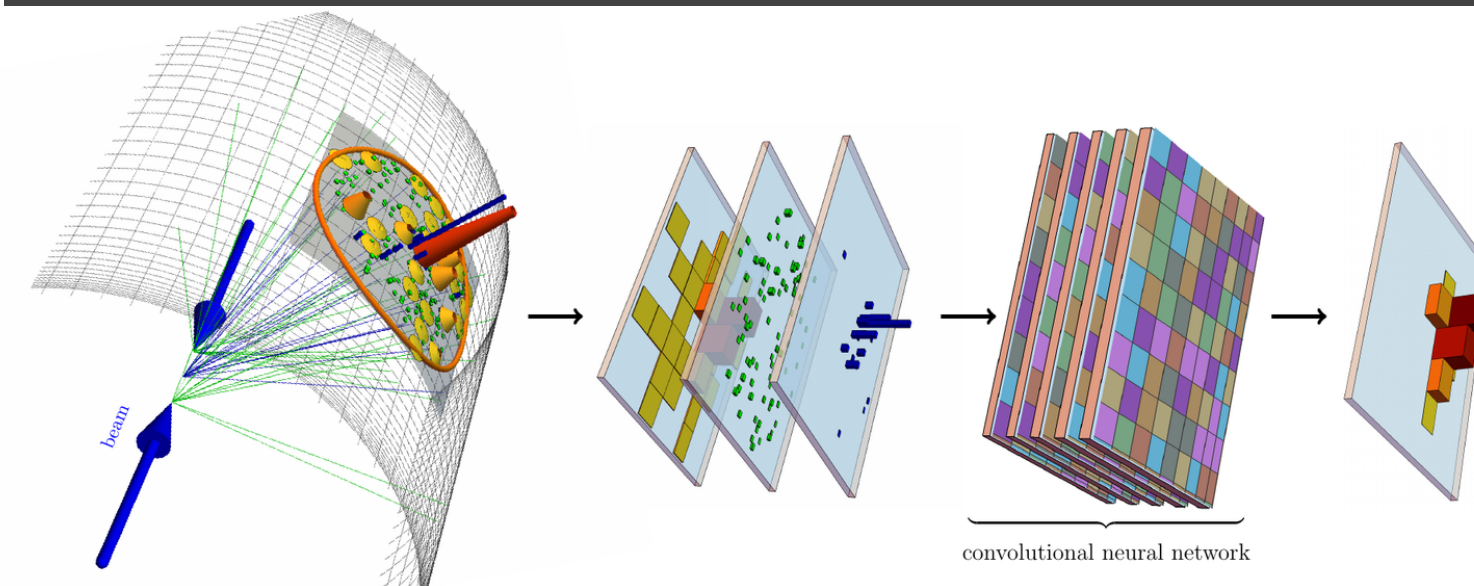


Collider
pheno

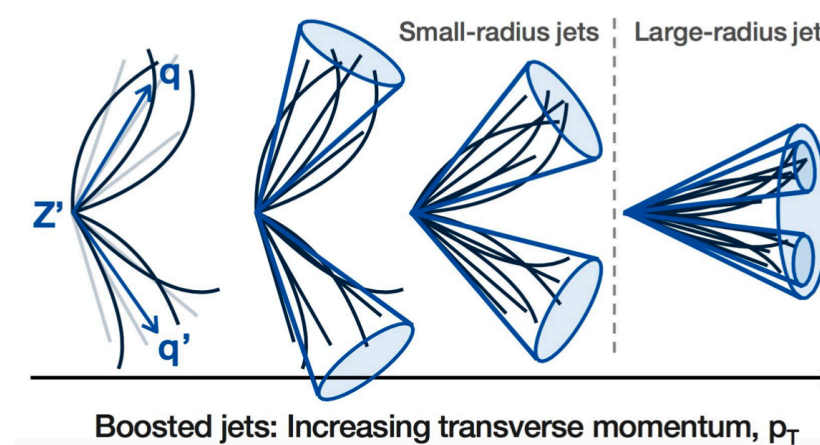
Non-perturbative QCD



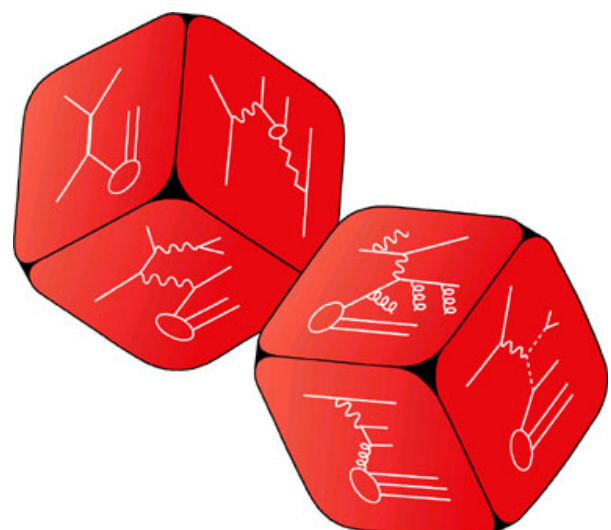
Novel strategies (e.g. ML, new observables)



BSM searches & jets



Event generators



The rich physics programme of the LHC

A central aspect is the search of new-physics (NP) phenomena, for which the LHC has set important constraints that forces us to think of some of the open questions from new angles...

e.g. scan for new phenomena (heavy new physics) within various models, with exclusion limits on NP scale

ATLAS Heavy Particle Searches* - 95% CL Upper Exclusion Limits

Status: March 2023

ATLAS Preliminary

$\int \mathcal{L} dt = (3.6 - 139) \text{ fb}^{-1}$ $\sqrt{s} = 13 \text{ TeV}$

Model	ℓ, γ	Jets [†]	E_T^{miss}	$\int \mathcal{L} dt [\text{fb}^{-1}]$	Limit	Reference	
Extra dimen.	ADD $G_{KK} + g/q$	0 e, μ, τ, γ	1-4 j	Yes	139	M_D 11.2 TeV $n=2$	2102.10874
	ADD non-resonant $\gamma\gamma$	2 γ	-	-	36.7	M_S 8.6 TeV $n=3$ HLZ NLO	1707.04147
	ADD QBH	-	2 j	-	139	M_{th} 9.4 TeV $n=6$	1910.08447
	ADD BH multijet	-	≥ 3 j	-	3.6	M_{th} 9.55 TeV $n=6, M_D=3 \text{ TeV, rot BH}$	1512.02586
	RS1 $G_{KK} \rightarrow \gamma\gamma$	2 γ	-	-	139	G_{KK} mass 4.5 TeV $k/\overline{M}_{Pl} = 0.1$	2102.13405
	Bulk RS $G_{KK} \rightarrow WW/ZZ$	multi-channel	-	-	36.1	G_{KK} mass 2.3 TeV $k/\overline{M}_{Pl} = 1.0$	1808.02380
	Bulk RS $g_{KK} \rightarrow tt$	1 e, μ	≥ 1 b, ≥ 1 J/2j	Yes	36.1	g_{KK} mass 3.8 TeV $\Gamma/m = 15\%$	1804.10823
	2UED / RPP	1 e, μ	≥ 2 b, ≥ 3 j	Yes	36.1	KK mass 1.8 TeV Tier (1,1), $\mathcal{B}(A^{(1,1)} \rightarrow tt) = 1$	1803.09678
Gauge bosons	SSM $Z' \rightarrow \ell\ell$	2 e, μ	-	-	139	Z' mass 5.1 TeV	1903.06248
	SSM $Z' \rightarrow \tau\tau$	2 τ	-	-	36.1	Z' mass 2.42 TeV	1709.07242
	Leptophobic $Z' \rightarrow bb$	-	2 b	-	36.1	Z' mass 2.1 TeV	1805.09299
	Leptophobic $Z' \rightarrow tt$	0 e, μ	≥ 1 b, ≥ 2 J	Yes	139	Z' mass 4.1 TeV $\Gamma/m = 1.2\%$	2005.05138
	SSM $W' \rightarrow \ell\nu$	1 e, μ	-	Yes	139	W' mass 6.0 TeV	1906.05609
	SSM $W' \rightarrow \tau\nu$	1 τ	-	Yes	139	W' mass 5.0 TeV	ATLAS-CONF-2021-025
	SSM $W' \rightarrow tb$	-	≥ 1 b, ≥ 1 J	-	139	W' mass 4.4 TeV	ATLAS-CONF-2021-043
	HVT $W' \rightarrow WZ$ model B	0-2 e, μ	2 j / 1 J	Yes	139	W' mass 4.3 TeV $g_V = 3$	2004.14636
	HVT $W' \rightarrow WZ \rightarrow \ell\nu\ell'\ell'$ model C	3 e, μ	2 j (VBF)	Yes	139	W' mass 340 GeV $g_{VCH} = 1, g_f = 0$	2207.03925
	HVT $Z' \rightarrow WW$ model B	1 e, μ	2 j / 1 J	Yes	139	Z' mass 3.9 TeV $g_V = 3$	2004.14636
LRSW $W_R \rightarrow \mu N_R$	2 μ	1 J	-	80	W_R mass 5.0 TeV $m(N_R) = 0.5 \text{ TeV, } g_L = g_R$	1904.12679	
CI	CI $qqqq$	-	2 j	-	37.0	Λ 21.8 TeV η_{LL}^-	1703.09127
	CI $\ell\ell qq$	2 e, μ	-	-	139	Λ 35.8 TeV η_{LL}^-	2006.12946
	CI $eebs$	2 e	1 b	-	139	Λ 1.8 TeV $g_* = 1$	2105.13847
	CI $\mu\mu bs$	2 μ	1 b	-	139	Λ 2.0 TeV $g_* = 1$	2105.13847
	CI $tttt$	≥ 1 e, μ	≥ 1 b, ≥ 1 j	Yes	36.1	Λ 2.57 TeV $ C_{4t} = 4\pi$	1811.02305
DM	Axial-vector med. (Dirac DM)	-	2 j	-	139	m_{med} 3.8 TeV	ATL-PHYS-PUB-2022-036
	Pseudo-scalar med. (Dirac DM)	0 e, μ, τ, γ	1-4 j	Yes	139	m_{med} 376 GeV	2102.10874
	Vector med. Z' -2HDM (Dirac DM)	0 e, μ	2 b	Yes	139	$m_{Z'}$ 3.0 TeV $\tan\beta=1, g_Z=0.8, m(\chi)=100 \text{ GeV}$	2108.13391
	Pseudo-scalar med. 2HDM+a	multi-channel	-	-	139	m_a 800 GeV $\tan\beta=1, g_\chi=1, m(\chi)=10 \text{ GeV}$	ATLAS-CONF-2021-036
LQ	Scalar LQ 1 st gen	2 e	≥ 2 j	Yes	139	LQ mass 1.8 TeV $\beta = 1$	2006.05872
	Scalar LQ 2 nd gen	2 μ	≥ 2 j	Yes	139	LQ mass 1.7 TeV $\beta = 1$	2006.05872
	Scalar LQ 3 rd gen	1 τ	2 b	Yes	139	LQ_3^u mass 1.49 TeV $\mathcal{B}(LQ_3^u \rightarrow b\tau) = 1$	2303.01294
	Scalar LQ 3 rd gen	0 e, μ	≥ 2 j, ≥ 2 b	Yes	139	LQ_3^d mass 1.24 TeV $\mathcal{B}(LQ_3^d \rightarrow \tau\nu) = 1$	2004.14060
	Scalar LQ 3 rd gen	≥ 2 $e, \mu, \geq 1$ $\tau, \geq 1$ j, ≥ 1 b	-	-	139	LQ_3^d mass 1.43 TeV $\mathcal{B}(LQ_3^d \rightarrow \tau\nu) = 1$	2101.11582
	Scalar LQ 3 rd gen	0 $e, \mu, \geq 1$ $\tau, 0-2$ j, 2 b	Yes	139	LQ_3^d mass 1.26 TeV $\mathcal{B}(LQ_3^d \rightarrow b\nu) = 1$	2101.12527	
	Vector LQ mix gen	multi-channel	≥ 1 j, ≥ 1 b	Yes	139	LQ_3^v mass 2.0 TeV $\mathcal{B}(\tilde{U}_1 \rightarrow t\mu) = 1, \text{Y-M coupl.}$	ATLAS-CONF-2022-052
	Vector LQ 3 rd gen	2 e, μ, τ	≥ 1 b	Yes	139	LQ_3^v mass 1.96 TeV $\mathcal{B}(LQ_3^v \rightarrow b\tau) = 1, \text{Y-M coupl.}$	2303.01294
Vector-like fermions	VLQ $TT \rightarrow Zt + X$	2 $e/2\mu \geq 3e, \mu$	≥ 1 b, ≥ 1 j	-	139	T mass 1.46 TeV	SU(2) doublet
	VLQ $BB \rightarrow Wt/Zb + X$	multi-channel	-	-	36.1	B mass 1.34 TeV	SU(2) doublet
	VLQ $T_{5/3} T_{5/3} T_{5/3} \rightarrow Wt + X$	2(SS) ≥ 3 e, μ	≥ 1 b, ≥ 1 j	Yes	36.1	$T_{5/3}$ mass 1.64 TeV $\mathcal{B}(T_{5/3} \rightarrow Wt) = 1, c(T_{5/3} Wt) = 1$	1807.11883
	VLQ $T \rightarrow Ht/Zt$	1 e, μ	≥ 1 b, ≥ 3 j	Yes	139	T mass 1.8 TeV	SU(2) singlet, $\kappa_T = 0.5$
	VLQ $Y \rightarrow Wb$	1 e, μ	≥ 1 b, ≥ 1 j	Yes	36.1	Y mass 1.85 TeV $\mathcal{B}(Y \rightarrow Wb) = 1, c_R(Wb) = 1$	1812.07343
	VLQ $B \rightarrow Hb$	0 e, μ	≥ 2 b, ≥ 1 j, ≥ 1 J	-	139	B mass 2.0 TeV	SU(2) doublet, $\kappa_B = 0.3$
	VLL $\tau' \rightarrow Z\tau/H\tau$	multi-channel	≥ 1 j	Yes	139	τ' mass 898 GeV	SU(2) doublet
Excited ferm.	Excited quark $q^* \rightarrow qg$	-	2 j	-	139	q^* mass 6.7 TeV	only u^* and $d^*, \Lambda = m(q^*)$
	Excited quark $q^* \rightarrow q\gamma$	1 γ	1 j	-	36.7	q^* mass 5.3 TeV	only u^* and $d^*, \Lambda = m(q^*)$
	Excited quark $b^* \rightarrow bg$	-	1 b, 1 j	-	139	b^* mass 3.2 TeV	1910.08447
	Excited lepton τ^*	2 τ	≥ 2 j	-	139	τ^* mass 4.6 TeV	$\Lambda = 4.6 \text{ TeV}$
Other	Type III Seesaw	2,3,4 e, μ	≥ 2 j	Yes	139	N^0 mass 910 GeV	2202.02039
	LRSW Majorana ν	2 μ	2 j	-	36.1	N_R mass 3.2 TeV	1809.11105
	Higgs triplet $H^{\pm\pm} \rightarrow W^\pm W^\pm$	2,3,4 e, μ (SS)	various	Yes	139	$H^{\pm\pm}$ mass 350 GeV	DY production
	Higgs triplet $H^{\pm\pm} \rightarrow \ell\ell$	2,3,4 e, μ (SS)	-	-	139	$H^{\pm\pm}$ mass 1.08 TeV	DY production
	Multi-charged particles	-	-	-	139	Multi-charged particle mass 1.59 TeV	DY production, $ q = 5e$
	Magnetic monopoles	-	-	-	34.4	monopole mass 2.37 TeV	DY production, $ g = 1g_D, \text{spin } 1/2$

$\sqrt{s} = 13 \text{ TeV}$ partial data $\sqrt{s} = 13 \text{ TeV}$ full data

*Only a selection of the available mass limits on new states or phenomena is shown.

†Small-radius (large-radius) jets are denoted by the letter j (J).

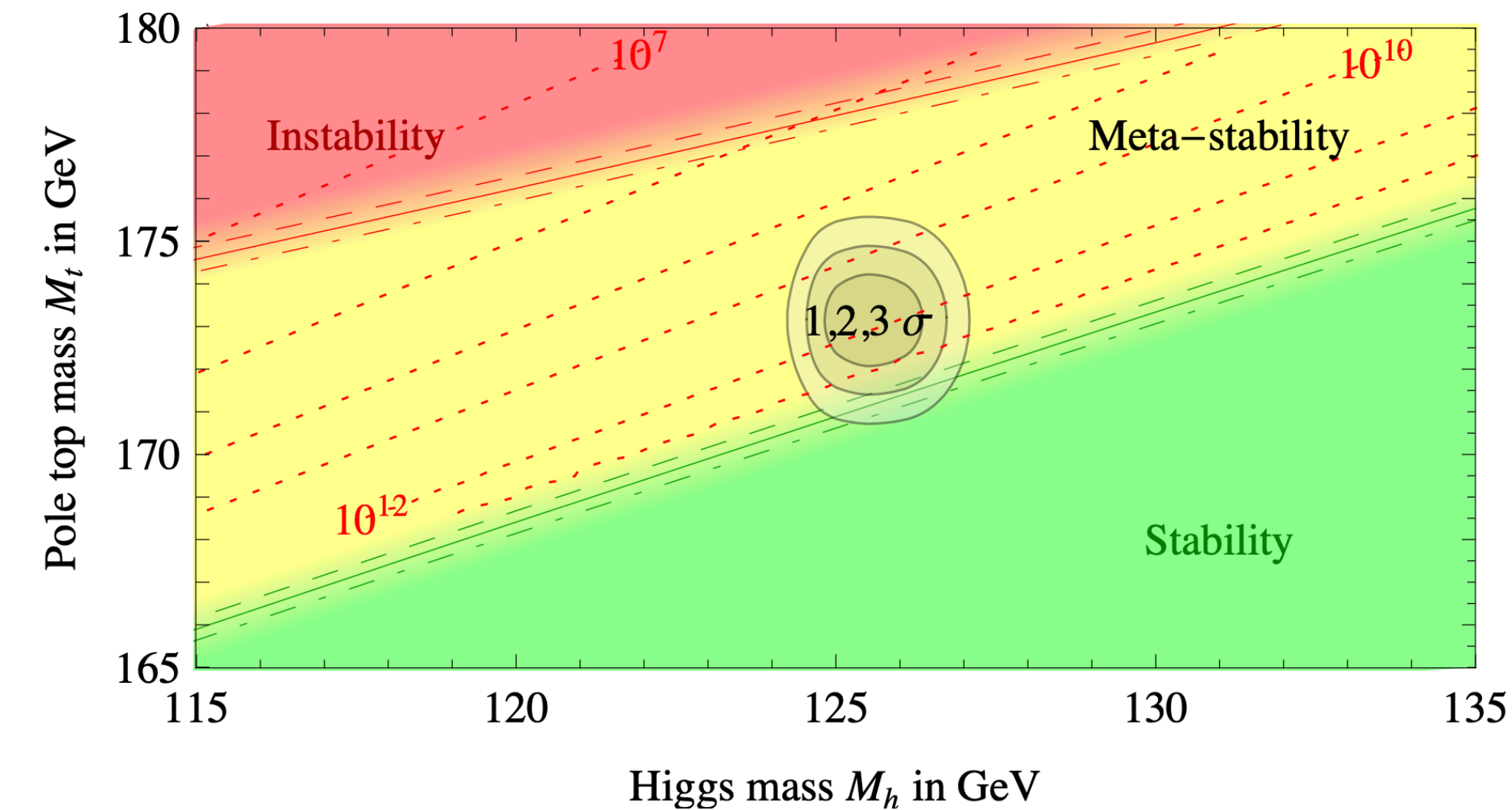
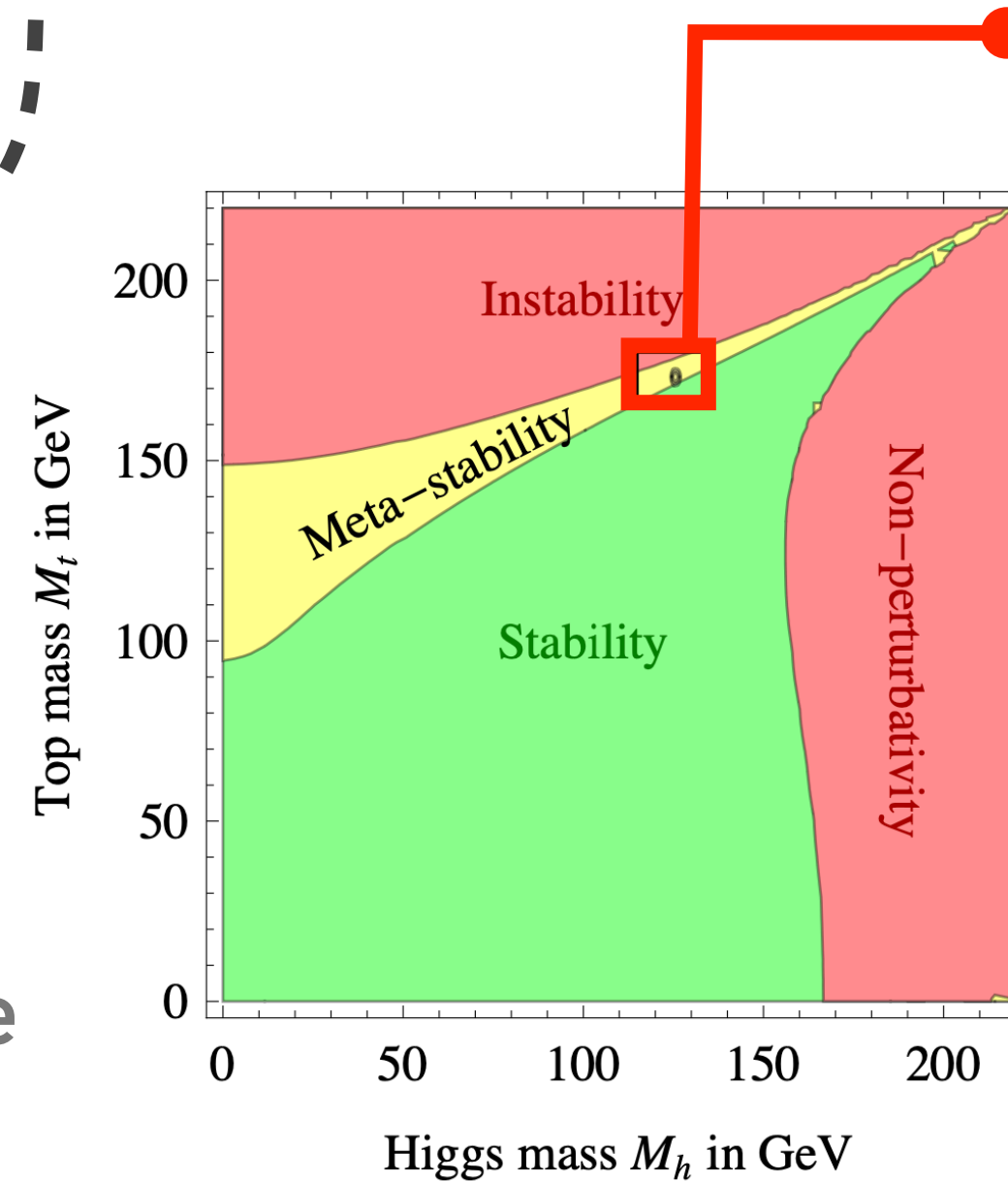
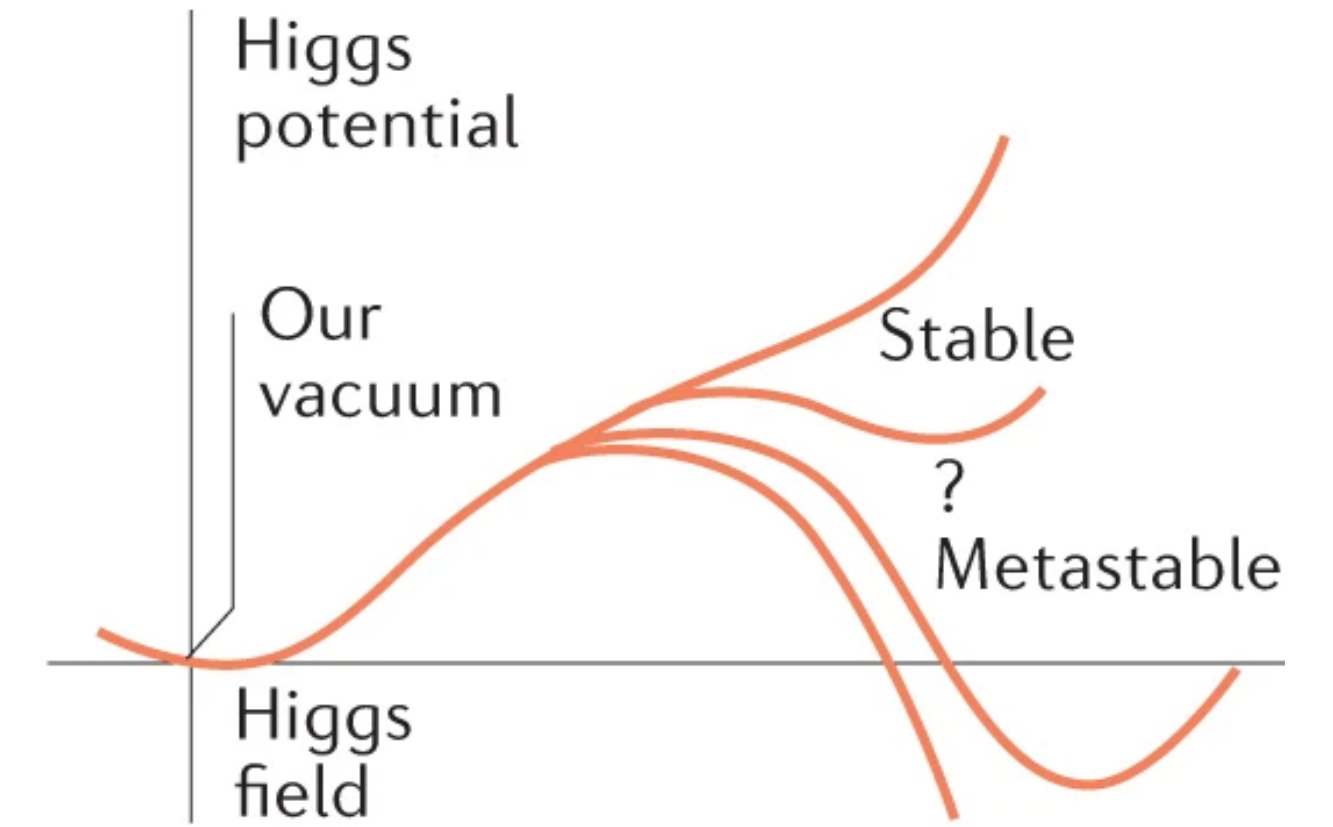
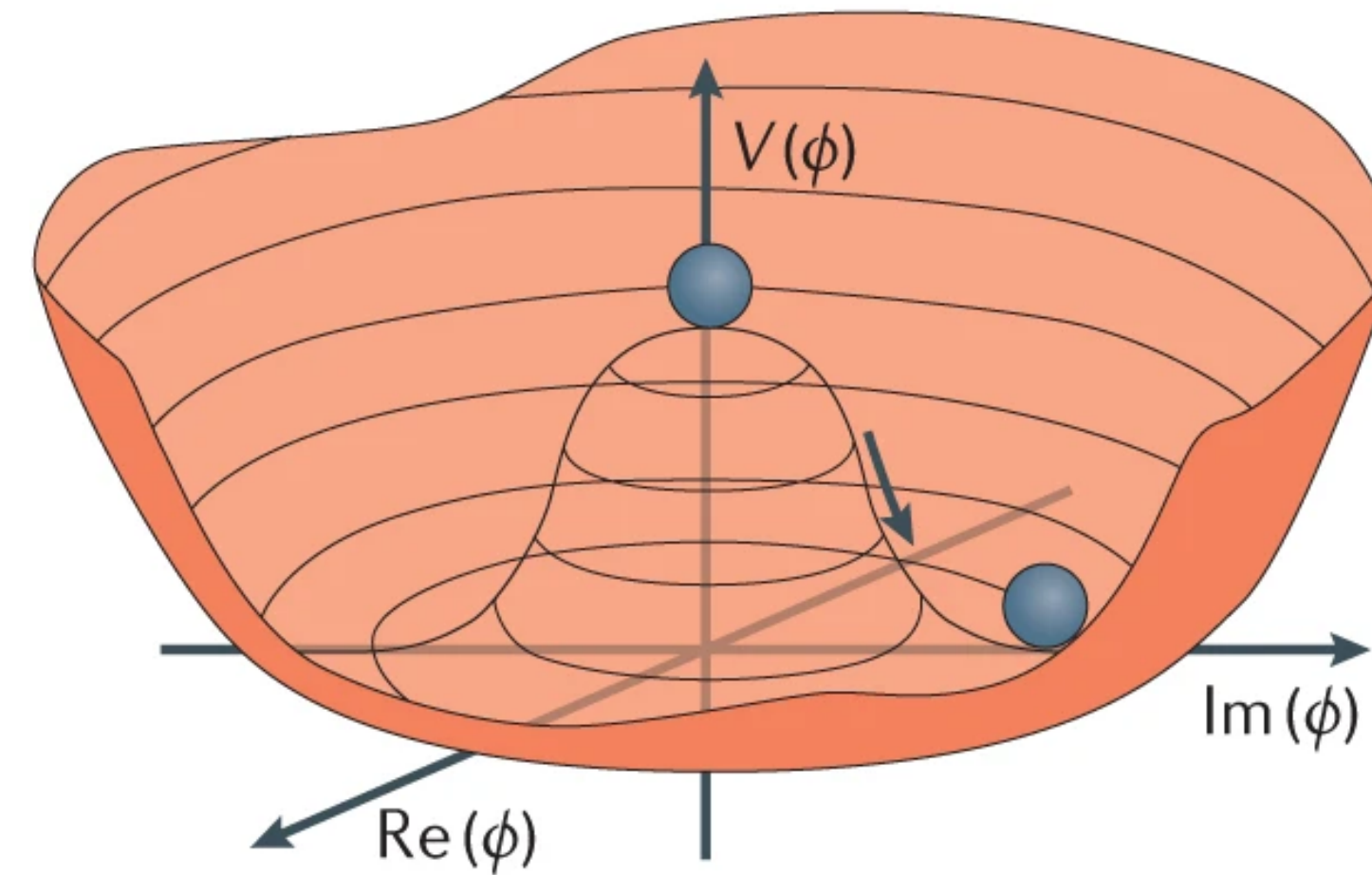
The rich physics programme of the LHC

Figures from 1205.6497 & 2104.06821

Another crucial element of the programme is precision physics. This provides an instrumental opportunity to a) study the fine structure of nature's QFTs, and b) exploit new creative ways of setting (indirect) constraints on NP models

$$V(\phi) = -\mu^2\phi^2 + \lambda\phi^4$$

e.g. precise measurements of the top and Higgs mass has direct implications on the stability of the vacuum of our universe



What makes the Higgs boson special?

- The Higgs boson plays a central role in this programme. Only fundamental (?) scalar observed so far
 - Mass of scalar particles not protected by symmetry arguments (e.g. like for gauge bosons), and can be as large as the theory cutoff (Planck scale M_{Planck} ?)

e.g. analogy with the pion (scalar, lightest hadron):

π mass is determined by the hadronic scale of the theory Λ (~ 300 MeV).

Why is the Higgs boson mass so much smaller than M_{Planck} ?



$$m_{\pi} \sim 130 - 140 \text{ MeV} \sim \Lambda$$



$$m_h \sim 125 \text{ GeV} \ll M_{\text{Planck}} (??)$$

What makes the Higgs boson special?

- The Higgs boson plays a central role in this programme. Only fundamental (?) scalar observed so far
 - Mass of scalar particles not protected by symmetry arguments (e.g. like for gauge bosons), and can be as large as the theory cutoff (Planck scale M_{Planck} ?)

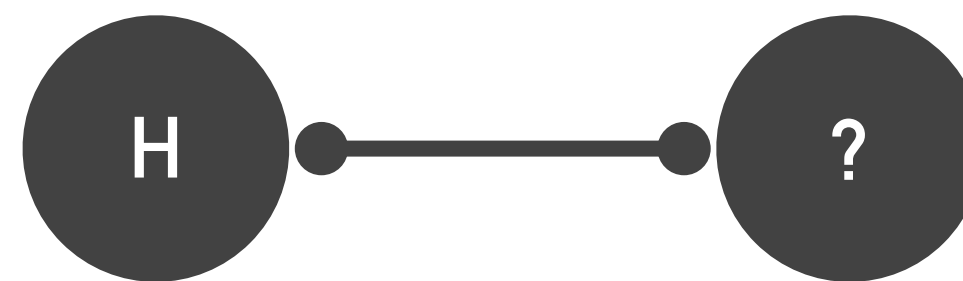
e.g. analogy with the pion (scalar, lightest hadron):

π mass is determined by the hadronic scale of the theory Λ (~ 300 MeV).

Why is the Higgs boson mass so much smaller than M_{Planck} ?



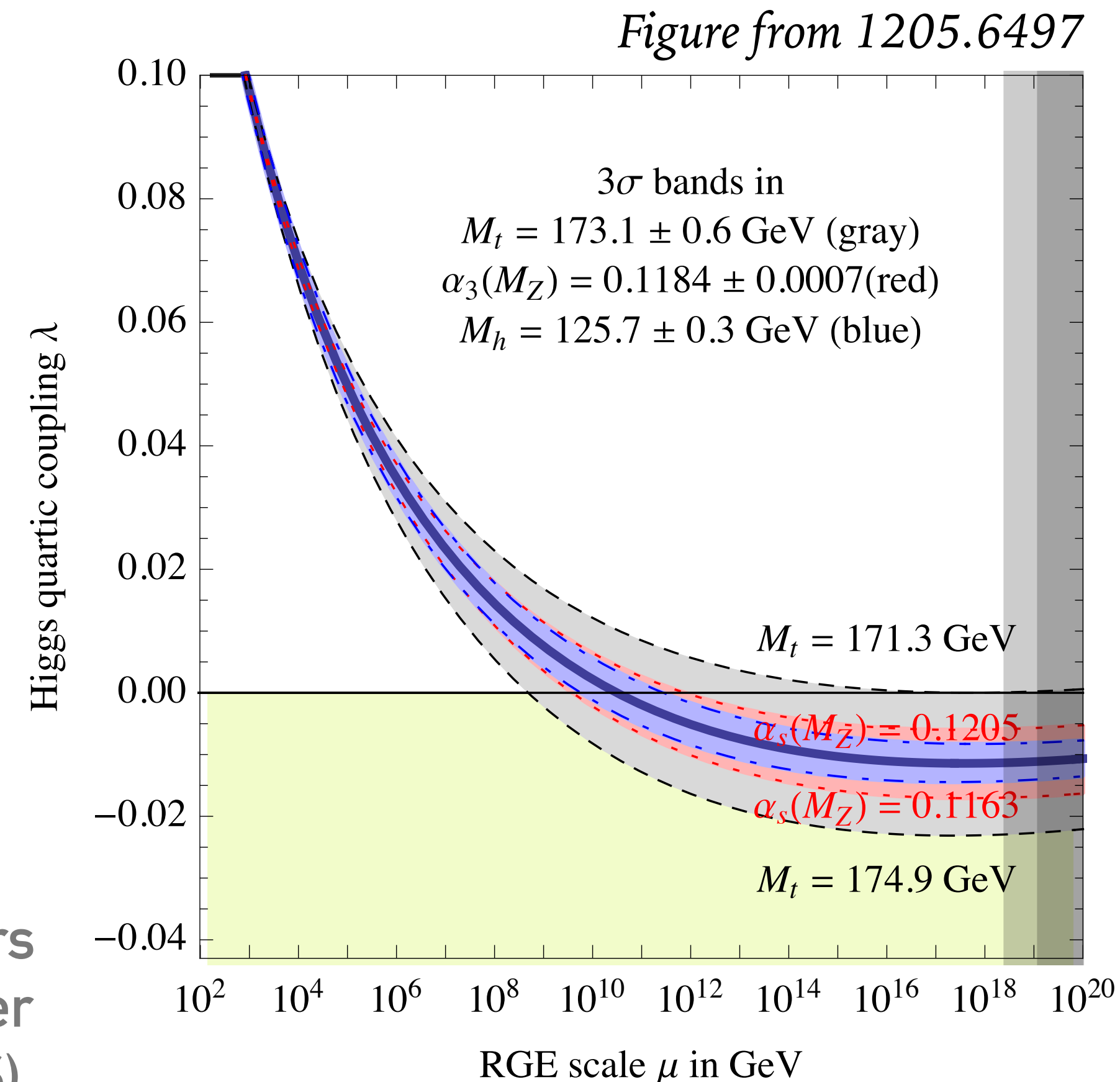
$$m_\pi \sim 130 - 140 \text{ MeV} \sim \Lambda$$



$$m_h \sim 125 \text{ GeV} \ll M_{\text{Planck}} (??)$$

- Evolution of SM Higgs' quartic interaction $\lambda(\mu)$ crosses zero at high energies, i.e. the H potential has other minima at large Higgs field and our vacuum will decay w/ very long lifetime (meta-stability)

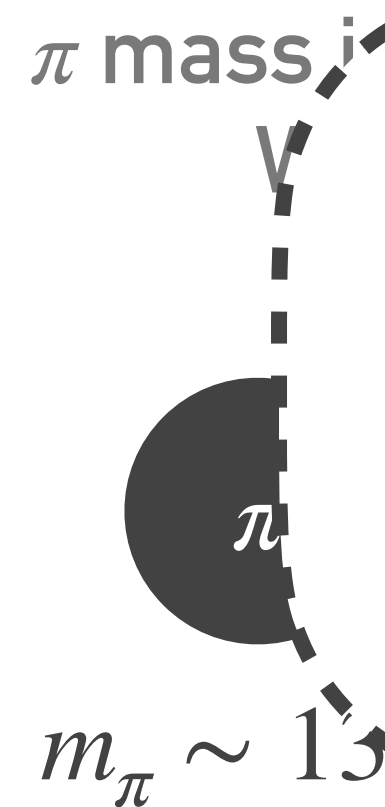
e.g. a somewhat similar behaviour is observed in (scalar) condensates of pairs of electrons in a superconducting material. In this case the scalar field (Cooper pairs) is just a low-energy manifestation of a more fundamental theory (BCS)



What makes the Higgs boson special?

- The Higgs boson plays a central role in this programme. Only fundamental (?) scalar observed so far
 - Mass of scalar particles not protected by symmetry arguments (e.g. like for gauge bosons), and can be as large as the theory cutoff (Planck scale M_{Planck} ?)

e.g. analogy with the pion (scalar, lightest hadron):

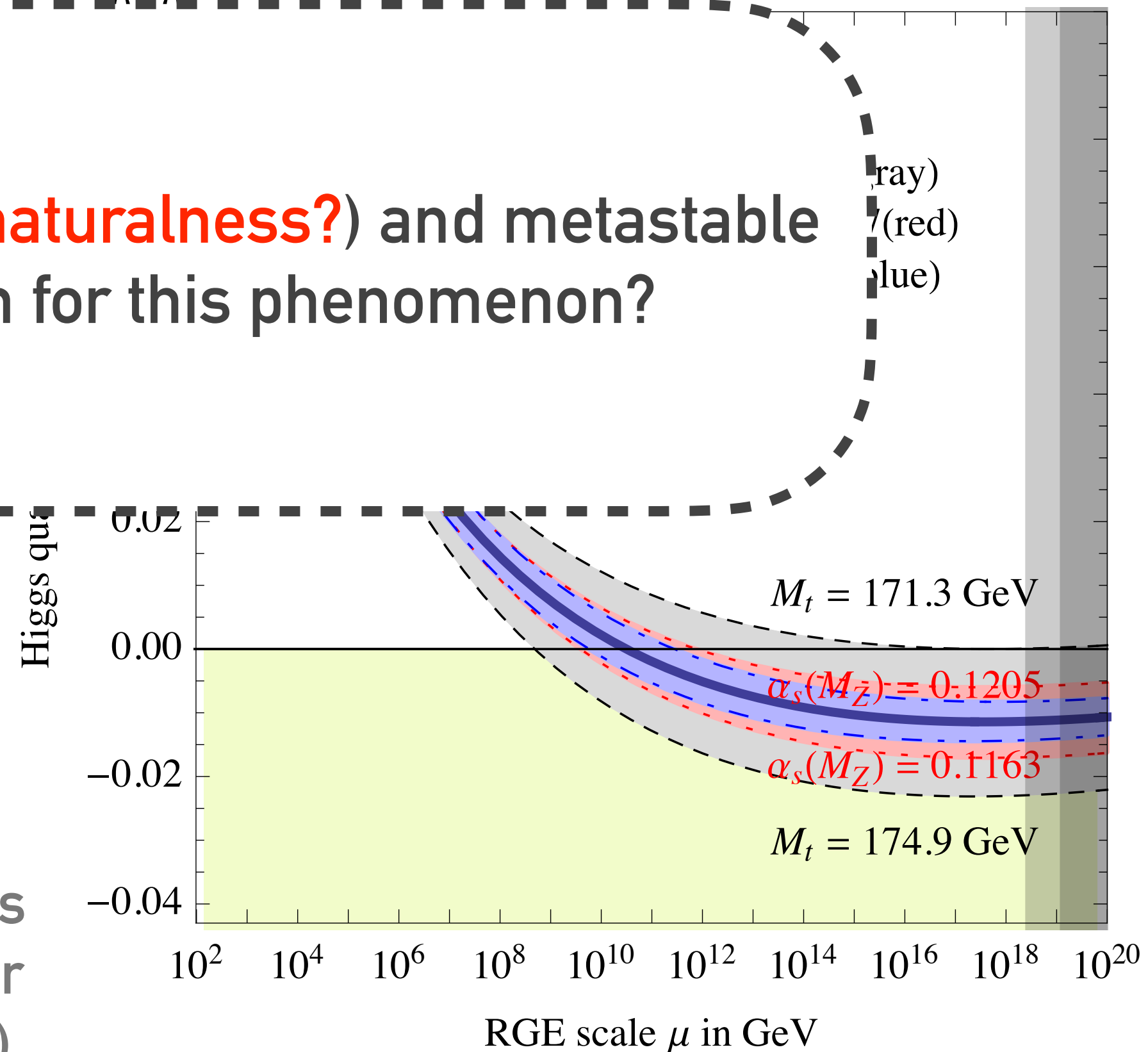


The Higgs boson indicates that we are living in a fine-tuned (**naturalness?**) and metastable universe (**criticality?**). Is there a microscopic explanation for this phenomenon?

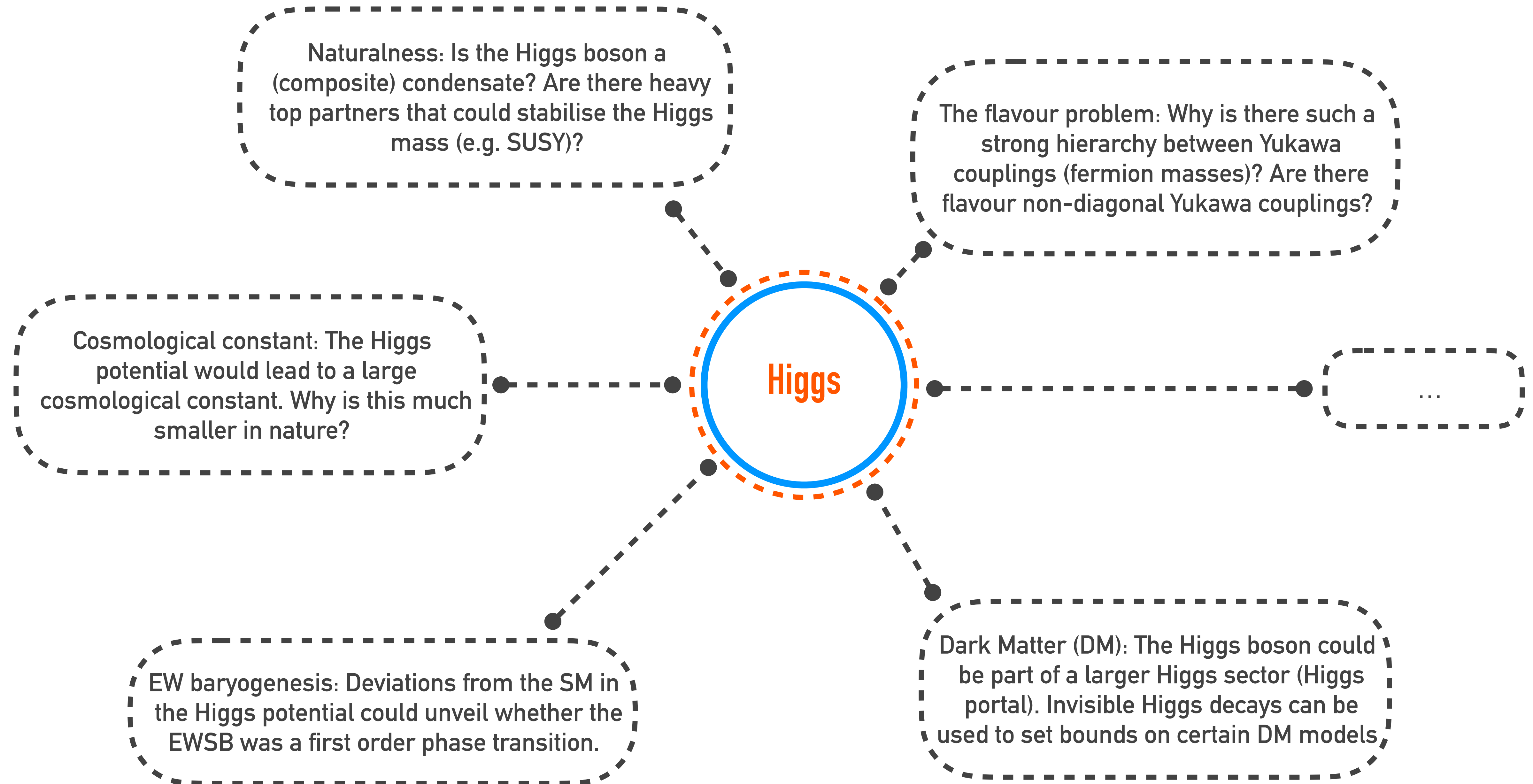
Figure from 1205.6497

- Evolution of SM Higgs' quartic interaction $\lambda(\mu)$ crosses zero at high energies, i.e. the H potential has other minima at large Higgs field and our vacuum will decay w/ very long lifetime (meta-stability)

e.g. a somewhat similar behaviour is observed in (scalar) condensates of pairs of electrons in a superconducting material. In this case the scalar field (Cooper pairs) is just a low-energy manifestation of a more fundamental theory (BCS)

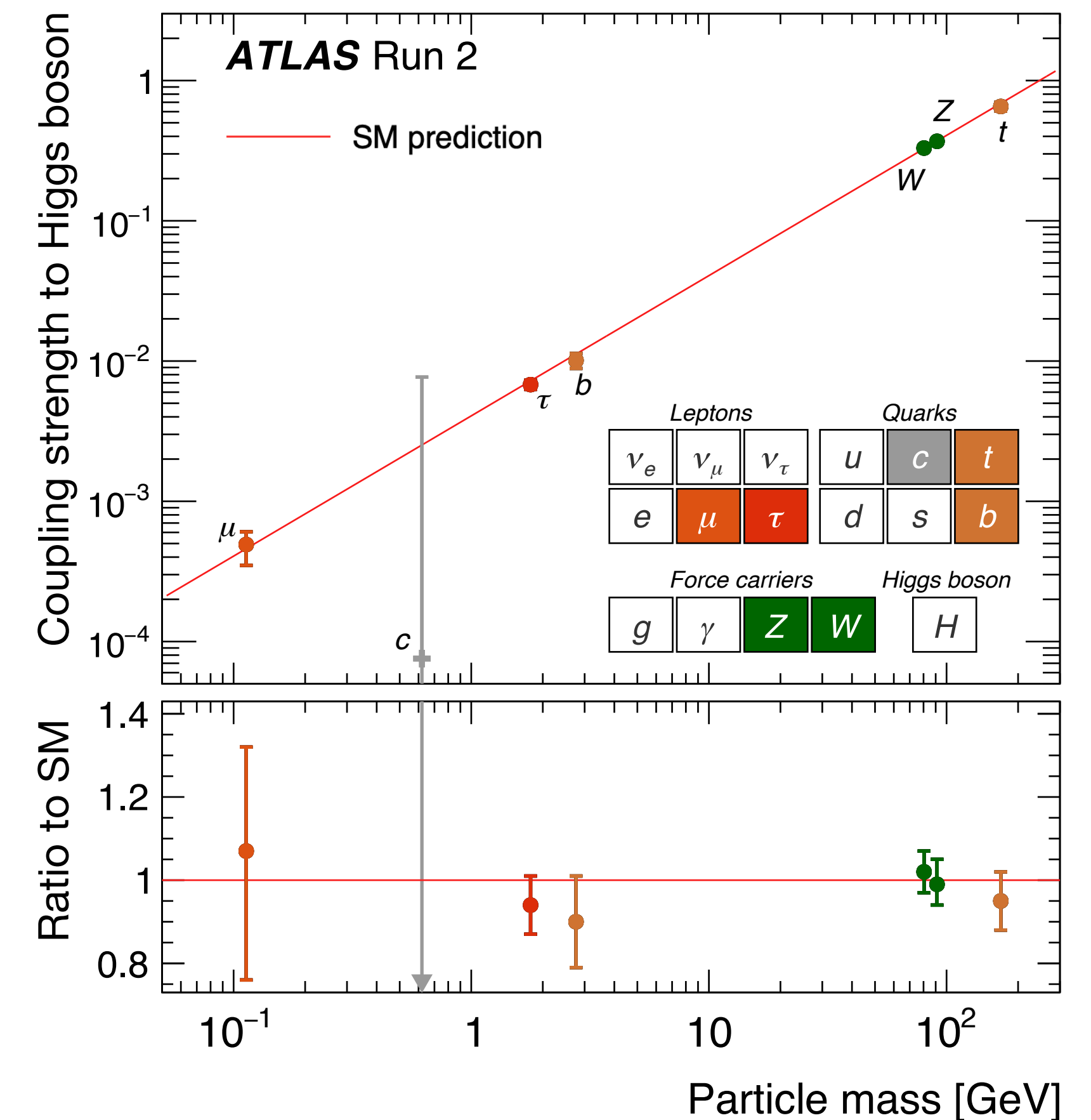
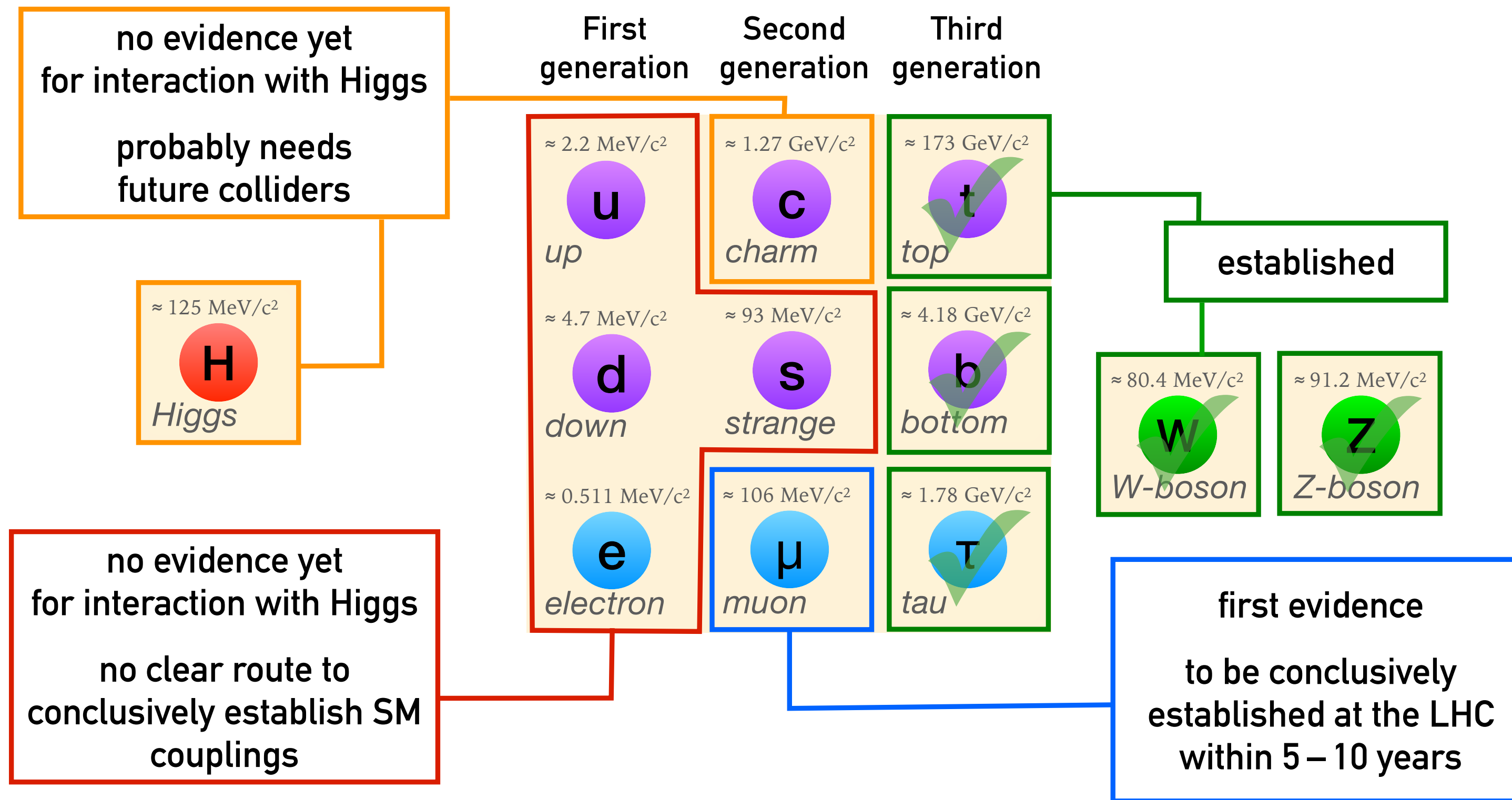


The Higgs boson's possible connection to (some) big open questions



Is it the SM Higgs boson? e.g. interaction with SM particles

- Interaction with EW bosons & 3rd generation fermions (Yukawa interactions) established to be SM like
- first exploration of some of 2nd generation Yukawa interactions ongoing

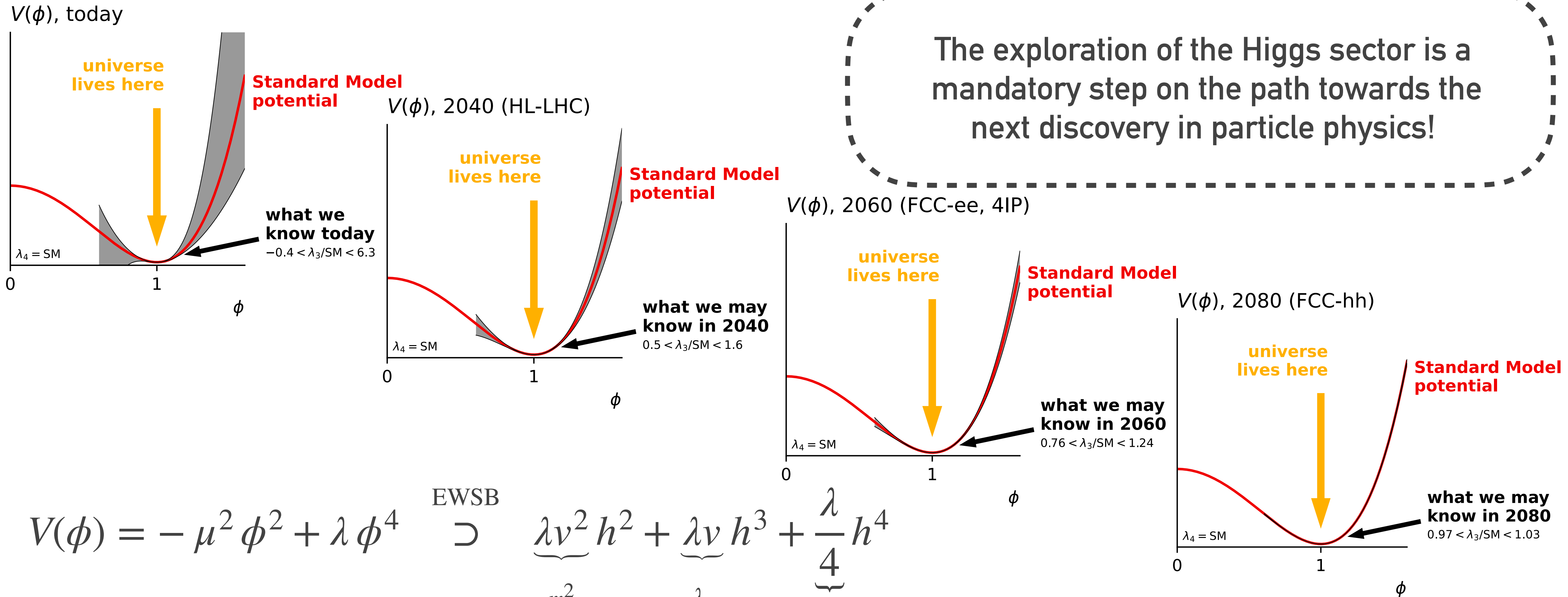


Is it the SM Higgs boson? e.g. the potential

Figures from G. Salam's talk at ICFA 2023

e.g. Display of current vs. future constraints on Higgs trilinear coupling (with $\lambda_4 = \text{SM}$)

The exploration of the Higgs sector is a mandatory step on the path towards the next discovery in particle physics!



$$V(\phi) = -\mu^2 \phi^2 + \lambda \phi^4 \quad \supset \quad \underbrace{\lambda v^2 h^2}_{\frac{m_h^2}{2}} + \underbrace{\lambda v h^3}_{\lambda_3} + \underbrace{\frac{\lambda}{4} h^4}_{\lambda_4}$$

Future colliders necessary for stringent constraints & direct measurement. Present LHC data shows $\lambda_3 \lesssim 6 \times \text{SM}$

At present not clear how to measure this

Goal of these lectures

Snapshots from: *Physics Letters B* 716 (2012) 1–29 (ATLAS)

Physics Letters B 716 (2012) 30–61 (CMS)

- The goal of these lectures is to explore the main concepts used in the theoretical description of collider events. We will take a learn-by-doing approach, using the Higgs boson as a concrete example

e.g. A few snapshots of the Higgs observation papers:

Samples of MC events used to represent signal and background are fully simulated using GEANT4 [103]. The simulations include pileup interactions matching the distribution of the number of such interactions observed in data. The description of the Higgs boson signal is obtained from MC simulation using, for most of the decay modes and production processes, the next-to-leading-order (NLO) matrix-element generator POWHEG [104,105], interfaced with PYTHIA 6.4 [106]. For the dominant gluon-gluon fusion process, the transverse momentum spectrum of the Higgs boson in the 7 TeV MC samples is reweighted to the next-to-next-to-leading-logarithmic (NNLL) + NLO distribution computed with HQT [71,72,107] and FEHiPRO [108,109], except in the $H \rightarrow ZZ$ analysis, where the effect is marginal. The agreement of the p_T spectrum in the simulation at 8 TeV with the NNLL + NLO distribution makes reweighting unnecessary. The improved agreement is due to a modification in the POWHEG setup recommended in Ref. [102]. The simulation of associated-production signal samples uses PYTHIA and all signal samples for $H \rightarrow bb$ are made using POWHEG interfaced to HERWIG++ [110]. Samples used for background studies are generated with PYTHIA, POWHEG, and MADGRAPH [111], and the normalisations are obtained from the best available NNLO or NLO calculations. The uncertainty in the signal cross section related to the choice of parton distribution functions is determined with the PDF4LHC prescription [96–100].

An exclusive category of events containing two jets improves the sensitivity to VBF. The other nine categories are defined by the presence or not of converted photons, η of the selected photons, and p_{Tt} , the component³ of the diphoton p_T that is orthogonal to the axis defined by the difference between the two photon momenta [99,100].

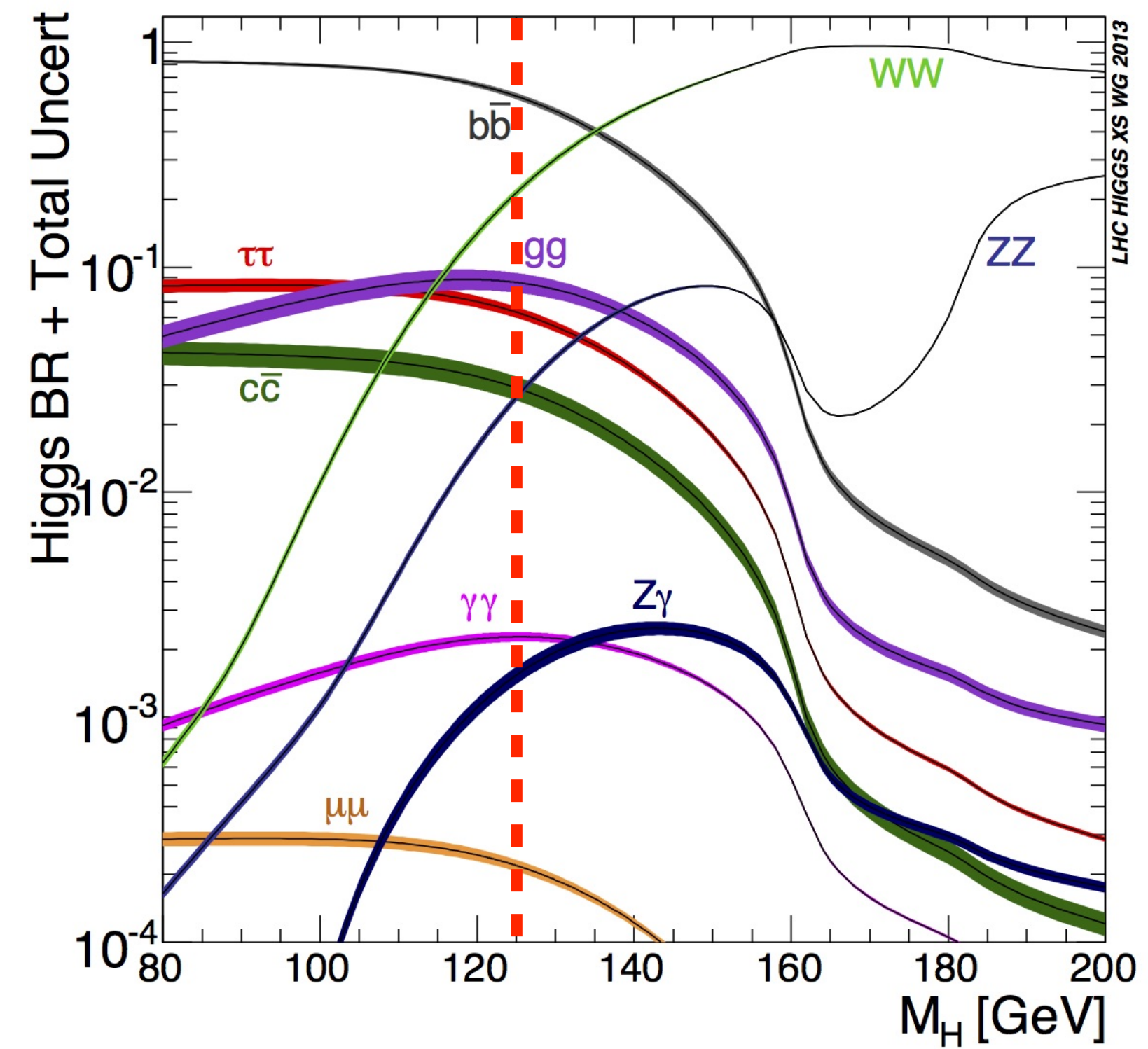
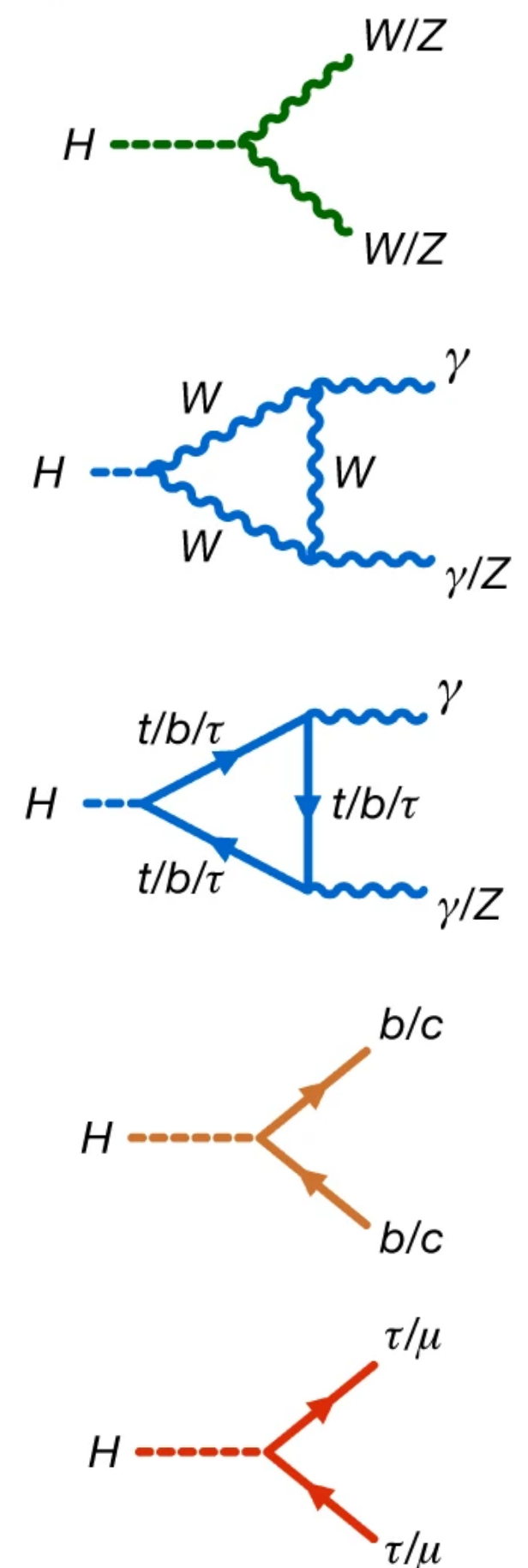
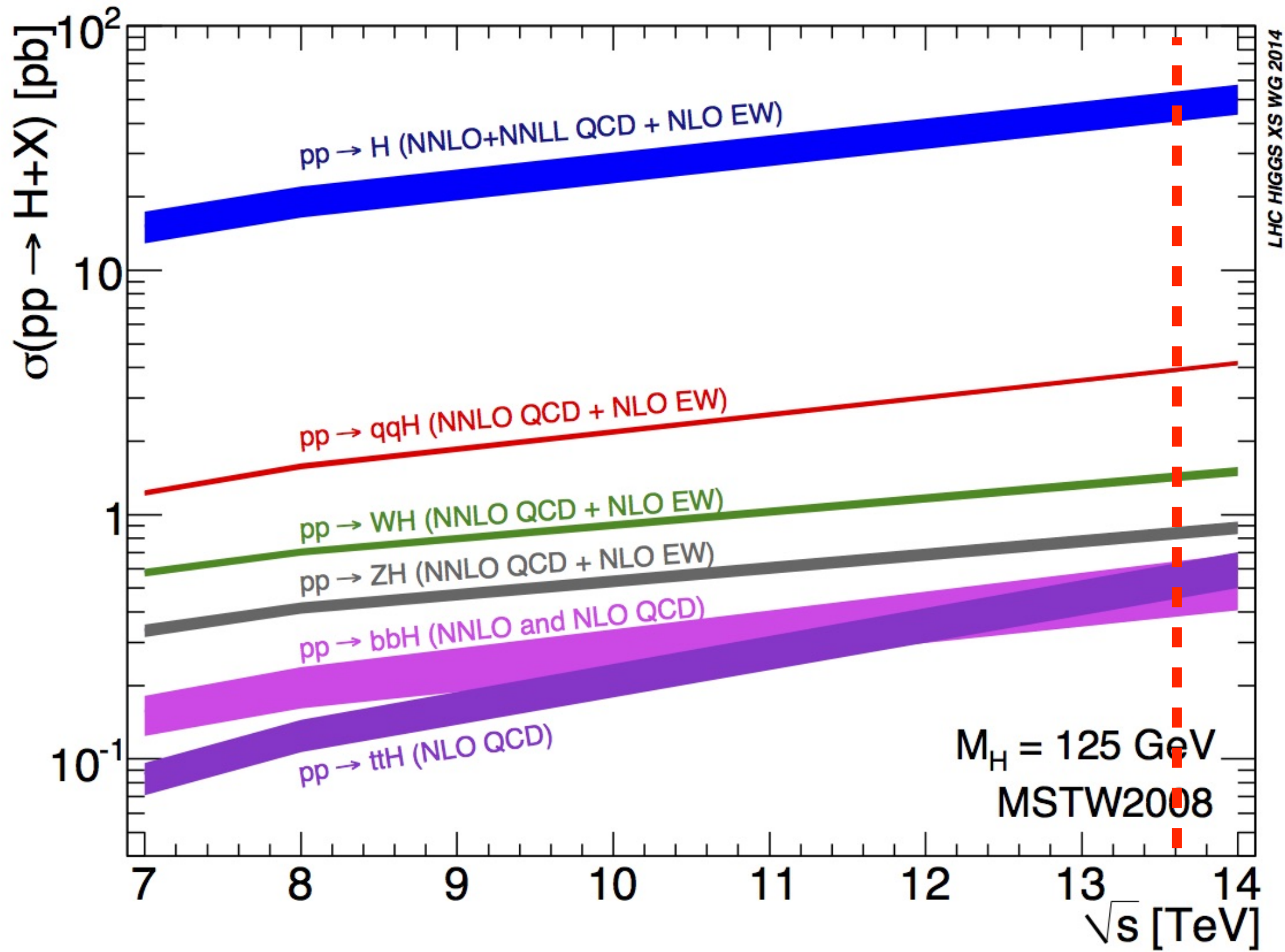
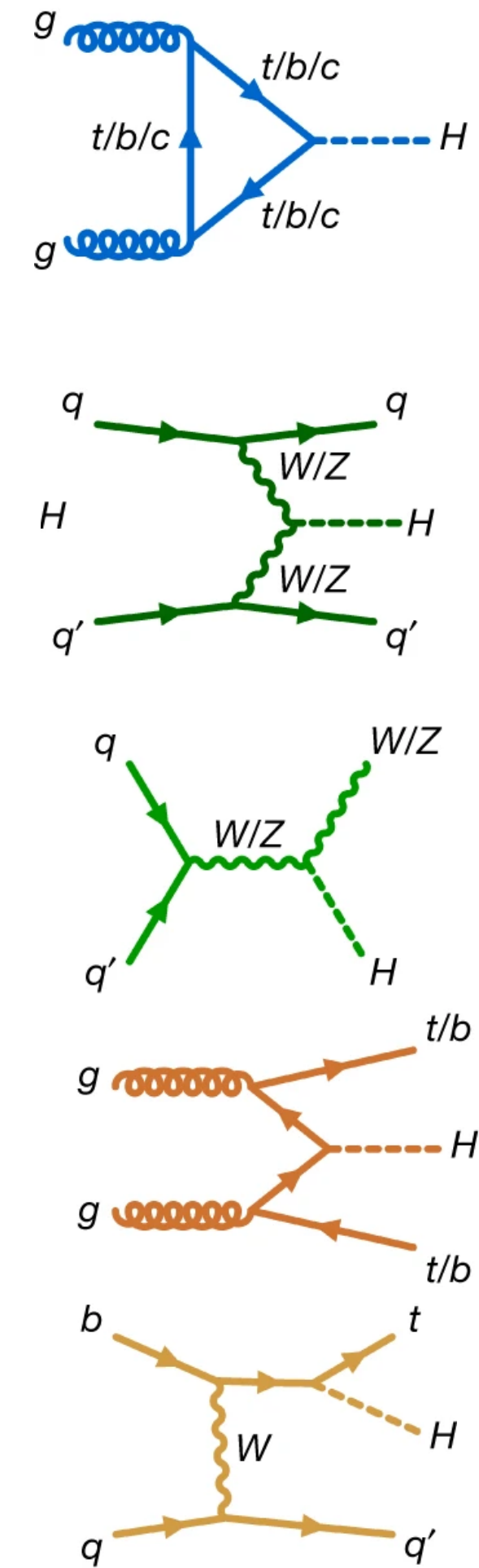
Jets are reconstructed [101] using the anti- k_t algorithm [102] with radius parameter $R = 0.4$. At least two jets with $|\eta| < 4.5$ and $p_T > 25$ GeV are required in the 2-jet selection. In the analysis of the 8 TeV data, the p_T threshold is raised to 30 GeV for jets with $2.5 < |\eta| < 4.5$.

The event generators used to model signal and background processes in samples of Monte Carlo (MC) simulated events are listed in Table 1. The normalisations of the generated samples are obtained from the state of the art calculations described above. Several different programs are used to generate the hard-scattering processes. To generate parton showers and their hadronisation, and to simulate the underlying event [66–68], PYTHIA6 [69] (for 7 TeV samples and 8 TeV samples produced with MadGraph [70,71] or AcerMC) or PYTHIA8 [72] (for other 8 TeV samples) are used. Alternatively, HERWIG [73] or SHERPA [74] are used to generate and hadronise parton showers, with the HERWIG underlying event simulation performed using JIMMY [75].

How to study the Higgs boson at the LHC

Feynman diagrams from 2207.00092

- Exploring the Higgs sector at the LHC demands an accurate control over hadronic events
 - Precise prediction for Higgs production and decay modes, as well as for background processes
 - e.g. total prodⁿ cross section and branching ratios:



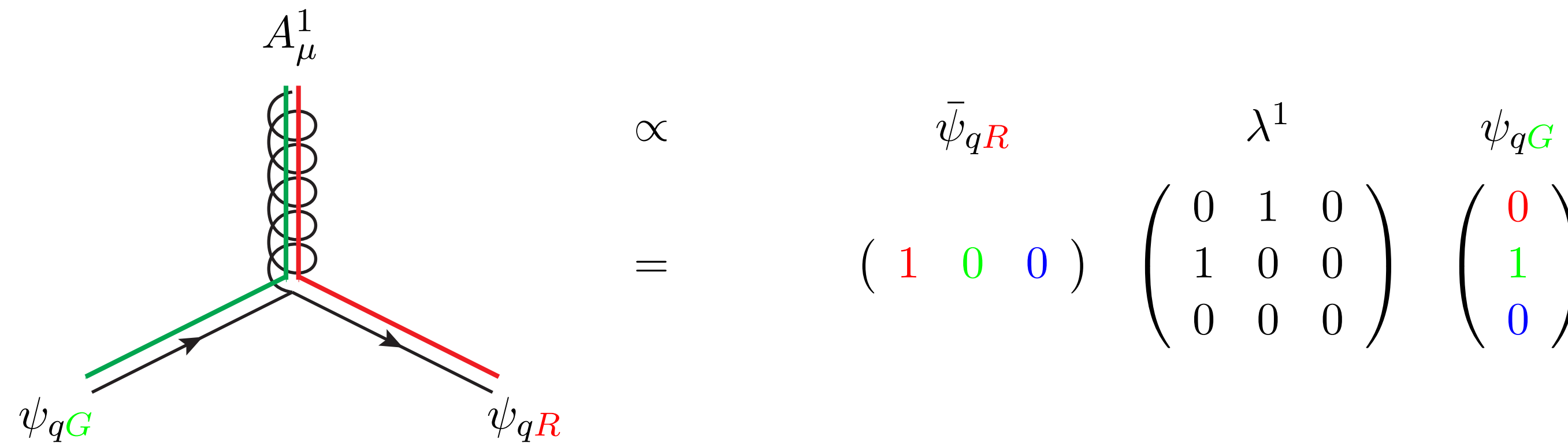
LHC events are shaped by strong interactions (QCD)

Vertex from Introduction to QCD 1207.2389

- General principles: $SU(3)_{\text{colour}}$ gauge invariance, Poincaré invariance (also causality, unitarity)

Quarks (fermions): Fundamental
 3 (quark), $\bar{3}$ (anti-quark) representation of $SU(3)_{\text{colour}}$
 (3 colour configurations)

Gluons (bosons): Adjoint representation of
 $SU(3)_{\text{colour}}$: $3 \oplus \bar{3} = 8 \oplus 1$
 (8 colour configurations)

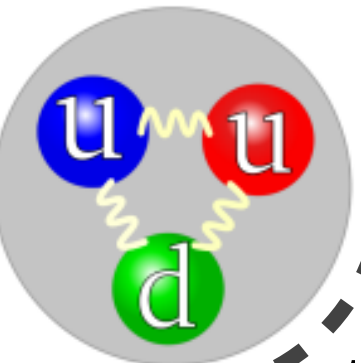


6 types (3 families):

1 st	2 nd	3 rd	Q/e
\underline{u}	\underline{c}	\underline{t}	$+\frac{2}{3}$
$m_u \simeq 0$	$m_c \simeq 1.3 \text{ GeV}$	$m_t \simeq 172.7 \text{ GeV}$	
\underline{d}	\underline{s}	\underline{b}	$-\frac{1}{3}$
$m_d \simeq 0$	$m_s \simeq 0$	$m_b \simeq 4.2 \text{ GeV}$	

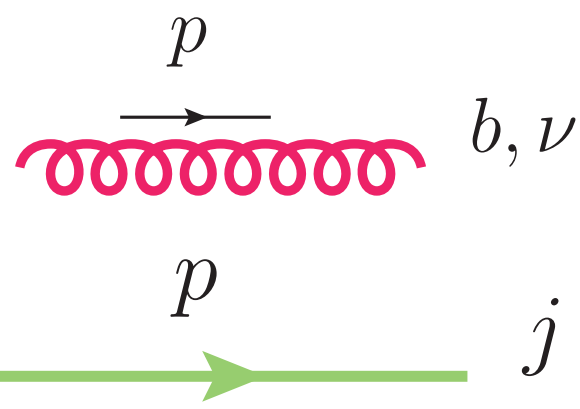
Confinement

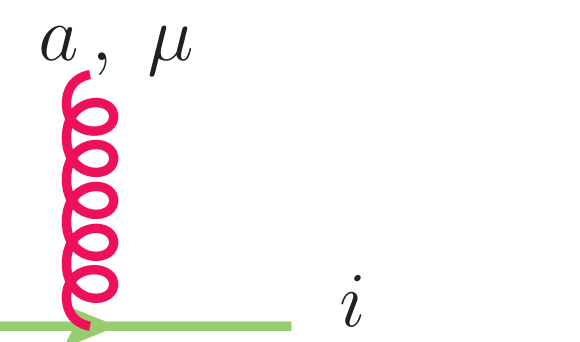
A key property is **confinement**: quarks & gluons not observed as free particles. They bind (Appendix) into colour-singlet hadrons:
 mesons: equal no. of quarks & anti-quarks (usually 1 pair),
 baryons: odd number of quarks (usually 3)
 (+ a sea of gluons and additional $q\bar{q}$ pairs)



The QCD Lagrangian

Feynman rules adapted from
Introduction to QCD and loop calculations G.Heinrich (TUM)

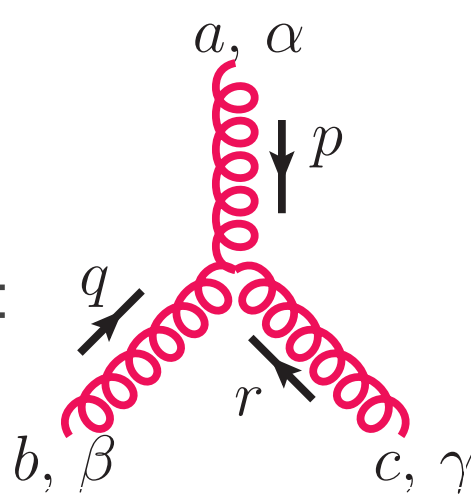
$$i\delta^{ij} \frac{\gamma_\mu p^\mu + m}{p^2 - m^2}$$


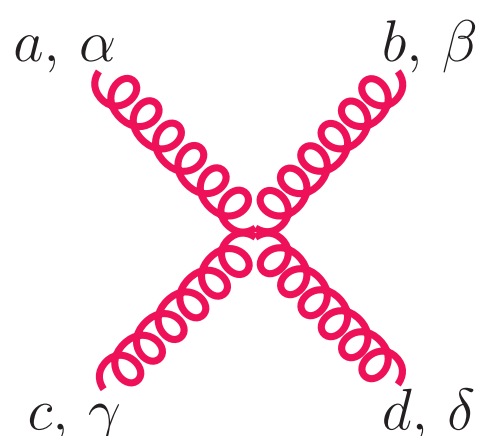
$$-i g_s (t^a)_{ij} \gamma^\mu$$


Unobserved, CP violating term, strong experimental bounds on θ (neutron electric dipole moment)

$$\mathcal{L}_{\text{QCD}} = -\frac{1}{4} F_{\mu\nu}^a F^{a,\mu\nu} + \sum_q \bar{\psi}_q (i\gamma_\mu D^\mu - m_q) \psi_q + \theta \frac{g_s^2}{64\pi^2} \epsilon^{\mu\nu\rho\sigma} F_{\mu\nu}^a F_{\rho\sigma}^a$$

$$(D^\mu)_{ab} = \delta_{ab} \partial^\mu + i g_s t_{ab}^c A^{c,\mu} \quad F_{\mu\nu}^c = \partial_\mu A_\nu^c - \partial_\nu A_\mu^c - g_s f^{abc} A_\mu^b A_\nu^c$$

$$-i g_s f^{abc} V_{\alpha\beta\gamma}(p, q, r)^\ddagger$$


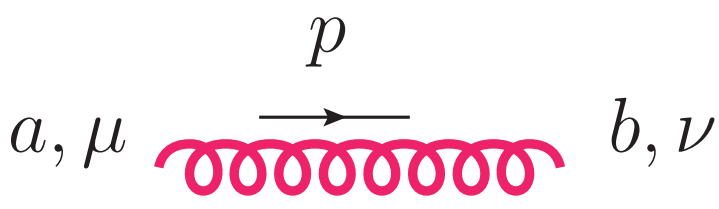
$$-i g_s^2 \begin{bmatrix} +f^{xac} f^{xbd} (g_{\alpha\beta} g_{\gamma\delta} - g_{\alpha\delta} g_{\beta\gamma}) \\ +f^{xad} f^{xcb} (g_{\alpha\gamma} g_{\beta\delta} - g_{\alpha\beta} g_{\gamma\delta}) \\ +f^{xab} f^{xdc} (g_{\alpha\delta} g_{\beta\gamma} - g_{\alpha\gamma} g_{\beta\delta}) \end{bmatrix}$$


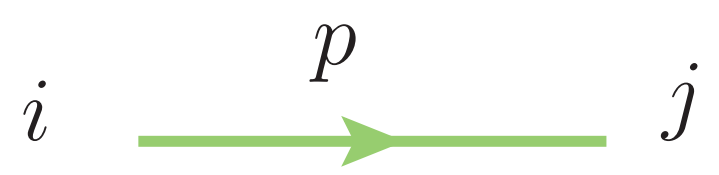
Non abelian gauge theory

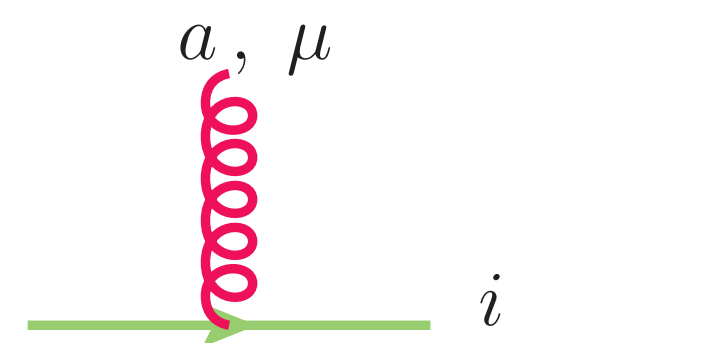
$\ddagger V_{\alpha\beta\gamma}(p, q, r) = (p - q)_\gamma g_{\alpha\beta} + (q - r)_\alpha g_{\beta\gamma} + (r - p)_\beta g_{\alpha\gamma}$

The QCD Lagrangian

Feynman rules adapted from
Introduction to QCD and loop calculations G.Heinrich (TUM)

$$\delta^{ab} \Delta_{\mu\nu}$$


$$i\delta^{ij} \frac{\gamma_\mu p^\mu + m}{p^2 - m^2}$$


$$-i g_s (t^a)_{ij} \gamma^\mu$$


Unobserved, CP violating term, strong experimental bounds on θ (neutron electric dipole moment)

$$\mathcal{L}_{\text{QCD}} = -\frac{1}{4} F_{\mu\nu}^a F^{a,\mu\nu} + \sum_q \bar{\psi}_q (i\gamma_\mu D^\mu - m_q) \psi_q + \theta \frac{g_s^2}{64\pi^2} \epsilon^{\mu\nu\rho\sigma} F_{\mu\nu}^a F_{\rho\sigma}^a$$

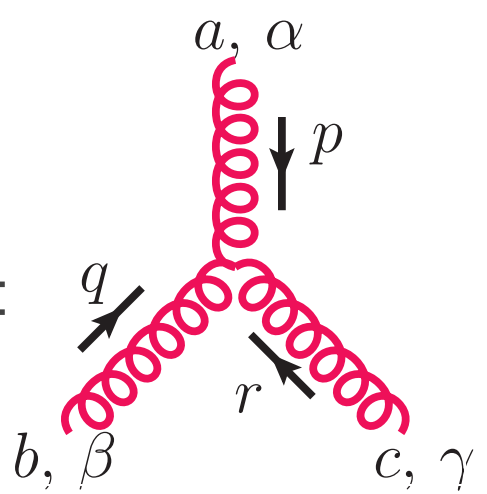
$$(D^\mu)_{ab} = \delta_{ab} \partial^\mu + i g_s t_{ab}^c A^{c,\mu} \quad F_{\mu\nu}^c = \partial_\mu A_\nu^c - \partial_\nu A_\mu^c - g_s f^{abc} A_\mu^b A_\nu^c$$

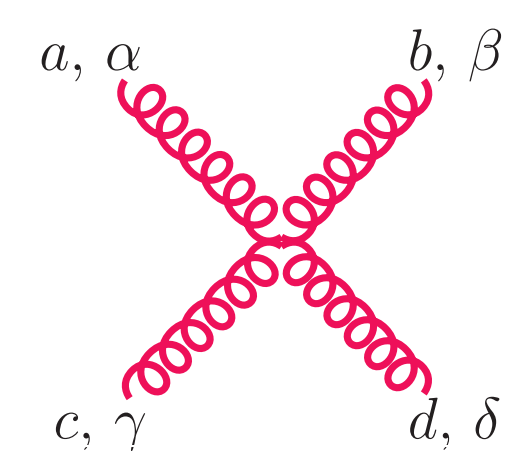
Basic colour algebra we'll use later

The emission of a gluon of colour c from a parton $i \in \{q, g\}$ is associated with a colour charge operator \mathbf{T}_i

$$(\mathbf{T}_i)_{ab}^c \equiv i f_{acb}, \quad i = g; \quad (\mathbf{T}_i)_{ab}^c \equiv t_{ab}^c, \quad i = q$$

$$\text{Tr}(t^a t^b) = \underbrace{\mathbf{T}_R}_{=1/2} \delta^{ab}, \quad \sum_{c,b} t_{ab}^c t_{bd}^c = \underbrace{\mathbf{C}_F}_{=4/3} \delta_{ad}, \quad \sum_{b,c} f_{abc} f_{dbc} = \underbrace{\mathbf{C}_A}_{=3} \delta_{ad}$$

$$-i g_s f^{abc} V_{\alpha\beta\gamma}(p, q, r)^\ddagger$$


$$-i g_s^2 \begin{bmatrix} +f^{xac} f^{xbd} (g_{\alpha\beta} g_{\gamma\delta} - g_{\alpha\delta} g_{\beta\gamma}) \\ +f^{xad} f^{xcb} (g_{\alpha\gamma} g_{\beta\delta} - g_{\alpha\beta} g_{\gamma\delta}) \\ +f^{xab} f^{xdc} (g_{\alpha\delta} g_{\beta\gamma} - g_{\alpha\gamma} g_{\beta\delta}) \end{bmatrix}$$


Non abelian gauge theory

Representation of SU(3) generators in terms of the Gell-Mann matrices (cf. Appendix)

$\ddagger V_{\alpha\beta\gamma}(p, q, r) = (p - q)_\gamma g_{\alpha\beta} + (q - r)_\alpha g_{\beta\gamma} + (r - p)_\beta g_{\alpha\gamma}$

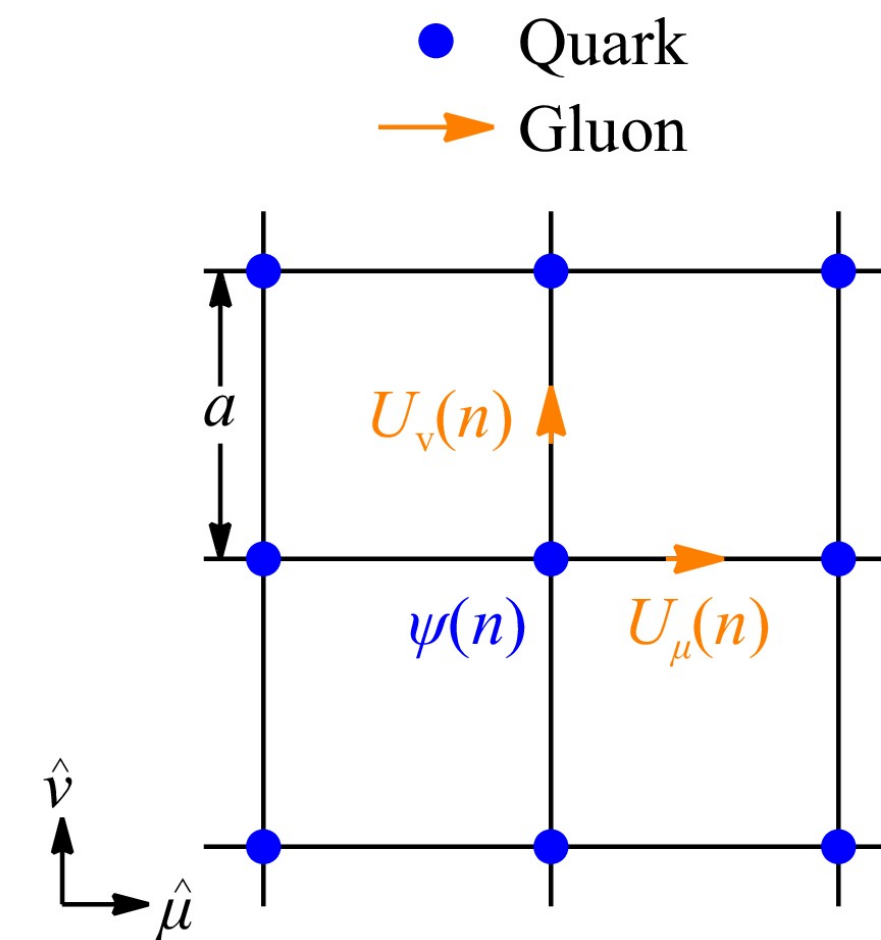
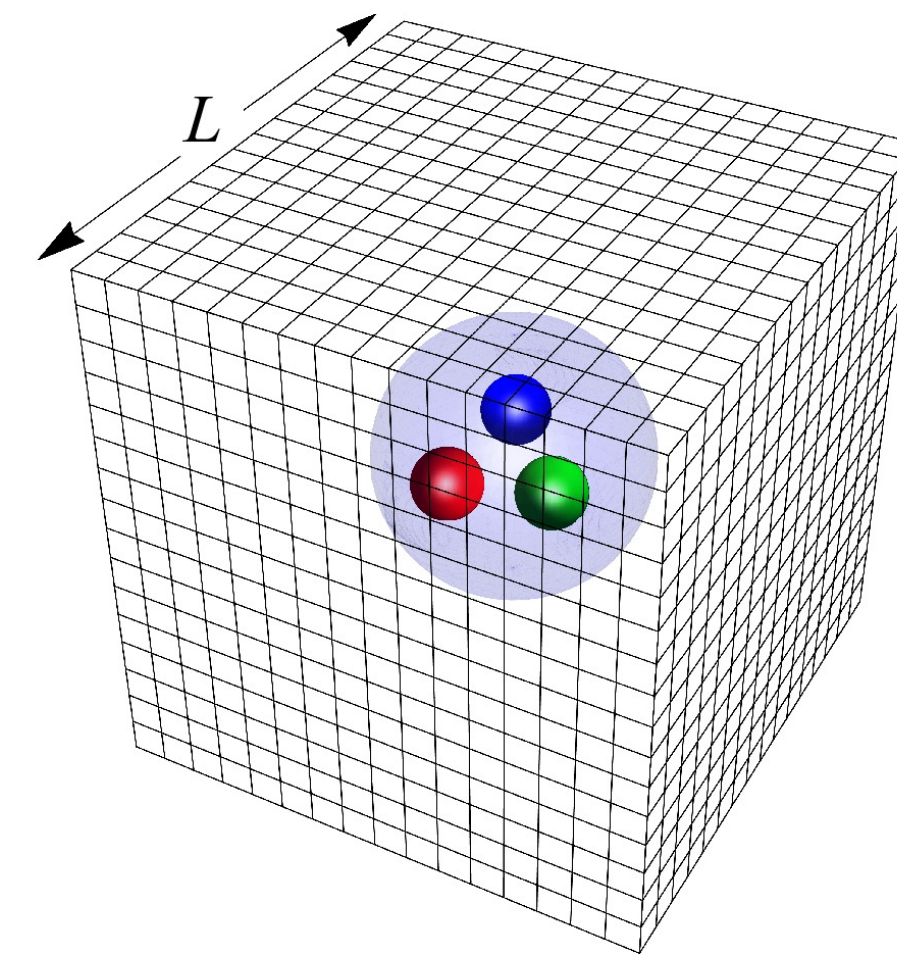
QCD for high-energy scattering

- Any observable (e.g. Green functions, S matrix from LSZ) can be obtained from the functional integral

$$\langle 0 | T G[A, \psi, \bar{\psi}] | 0 \rangle = \mathcal{N} \int \mathcal{D}A \mathcal{D}\psi \mathcal{D}\bar{\psi} e^{i \int d^4x \mathcal{L}(x)} G[A, \psi, \bar{\psi}]$$

● Functional of the QCD fields (e.g. $G = F_{\mu\nu} F^{\mu\nu} \bar{\psi} \psi$)
 ● Time ordering
 ● Vacuum

NB: including gauge fixing and Faddeev-Popov Lagrangians necessary to keep formulation well defined



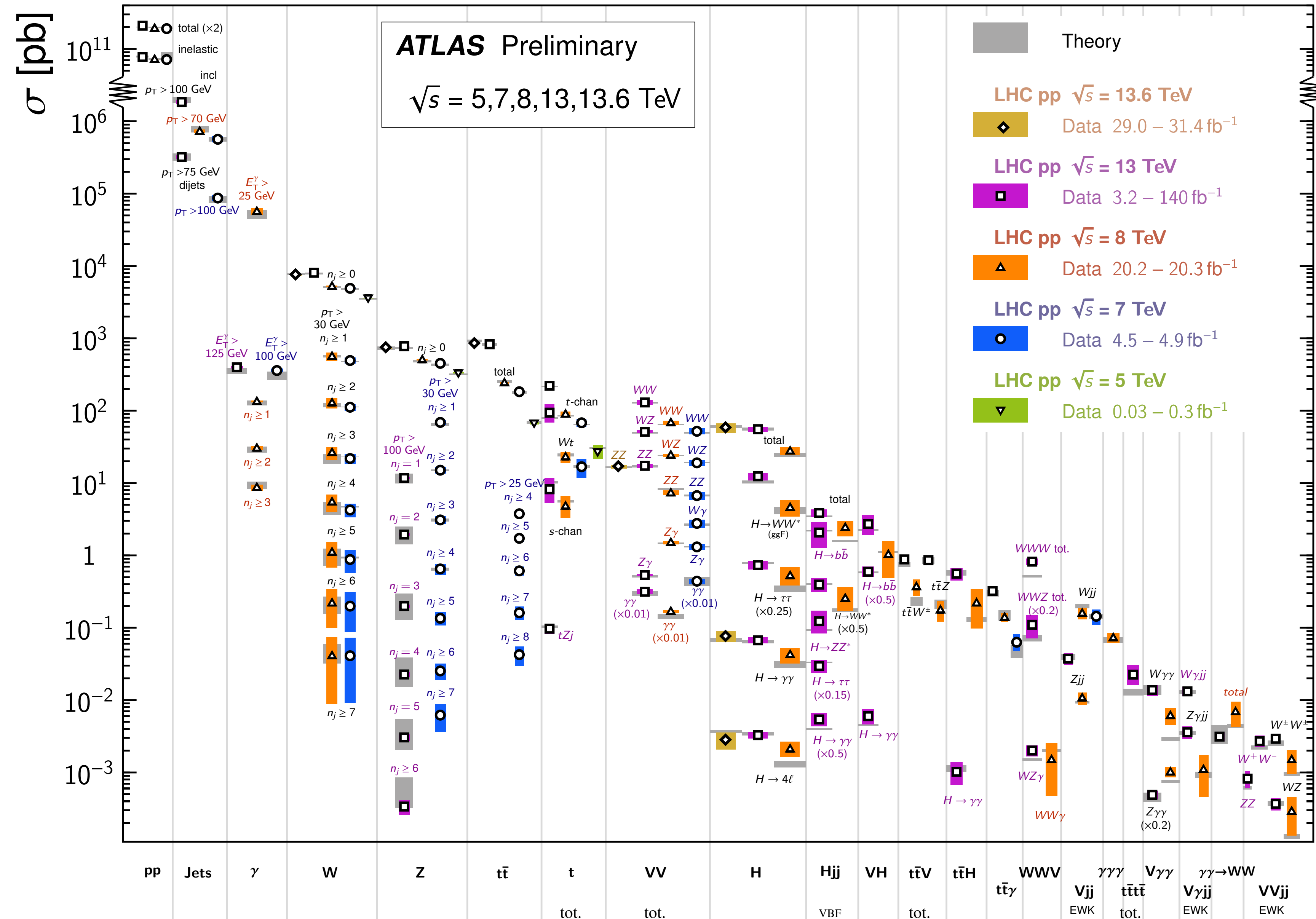
- Contains full information about the theory, but extremely hard to solve exactly. An exception is given by lattice methods, although describing a scattering process is **unfeasible** at present (Minkowskian problem, enormous lattice size required)

- In practice we resort to perturbative methods, i.e. solve integral for the free theory (simple!) and then account for interacting Lagrangian as **perturbations** around the free-theory solution

Great success of perturbation theory at the LHC

Status: June 2024

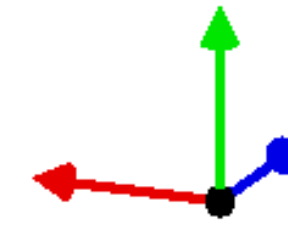
Standard Model Production Cross Section Measurements



Remarkable agreement with experimental data for broad range of reactions (multiple orders of magnitude in cross section units)!

A realistic LHC event: e.g. dilepton (Drell-Yan) production

CMS Experiment at LHC, CERN
Data recorded: Sat Aug 22 04:13:48 2015 CEST
Run/Event: 254833 / 1268846022
Lumi section: 846



Electron 1,
pt = 1278.63
eta = -1.312
phi = 0.420

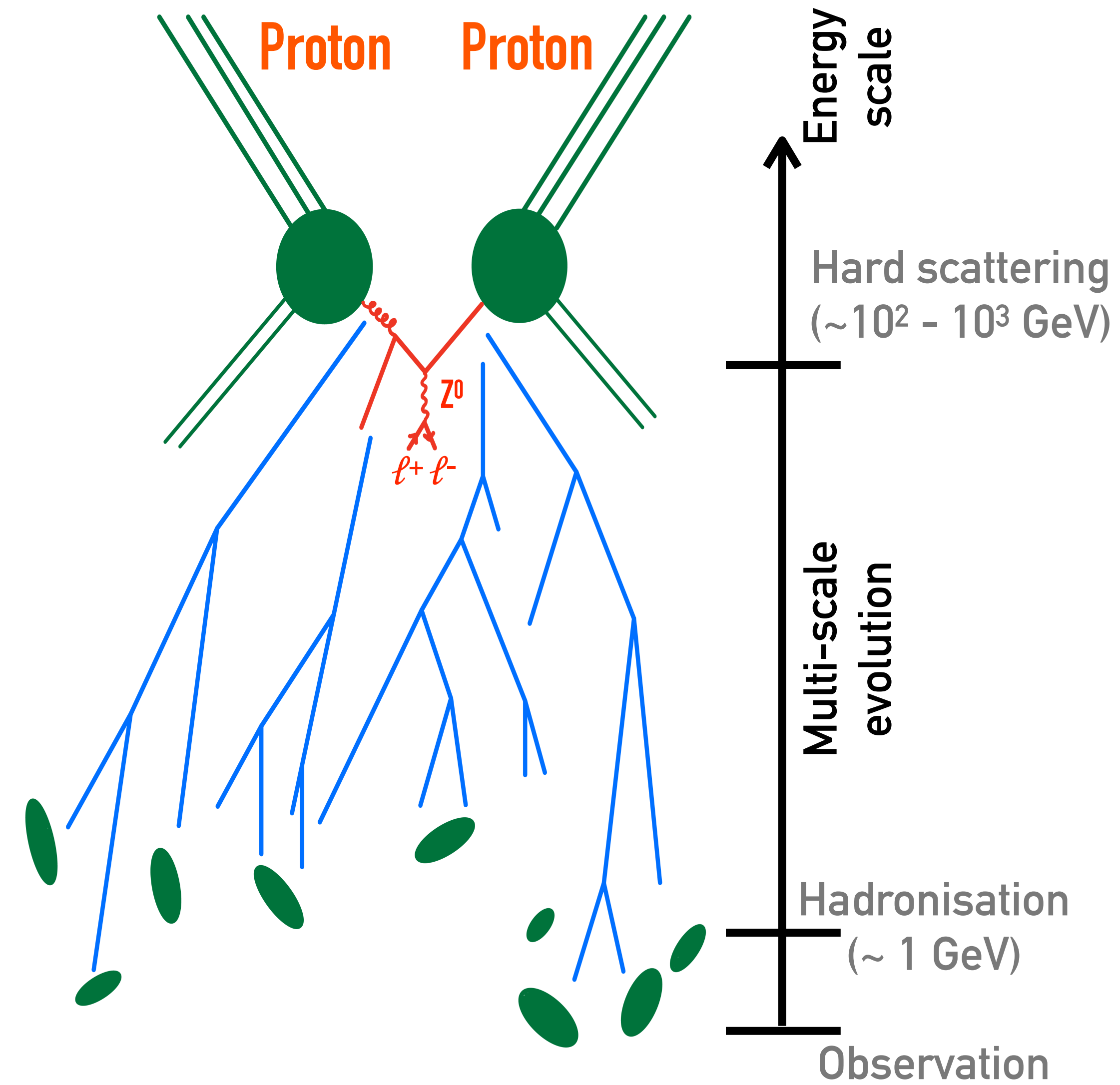
Electron 0,
pt = 1256.20
eta = -0.239
phi = -2.741

Complexity of hadronic scattering

Each event is the result of multiple pp collisions per bunch crossing (**pile up**), and each pp collision involves several simultaneous scatterings (**MPI**)



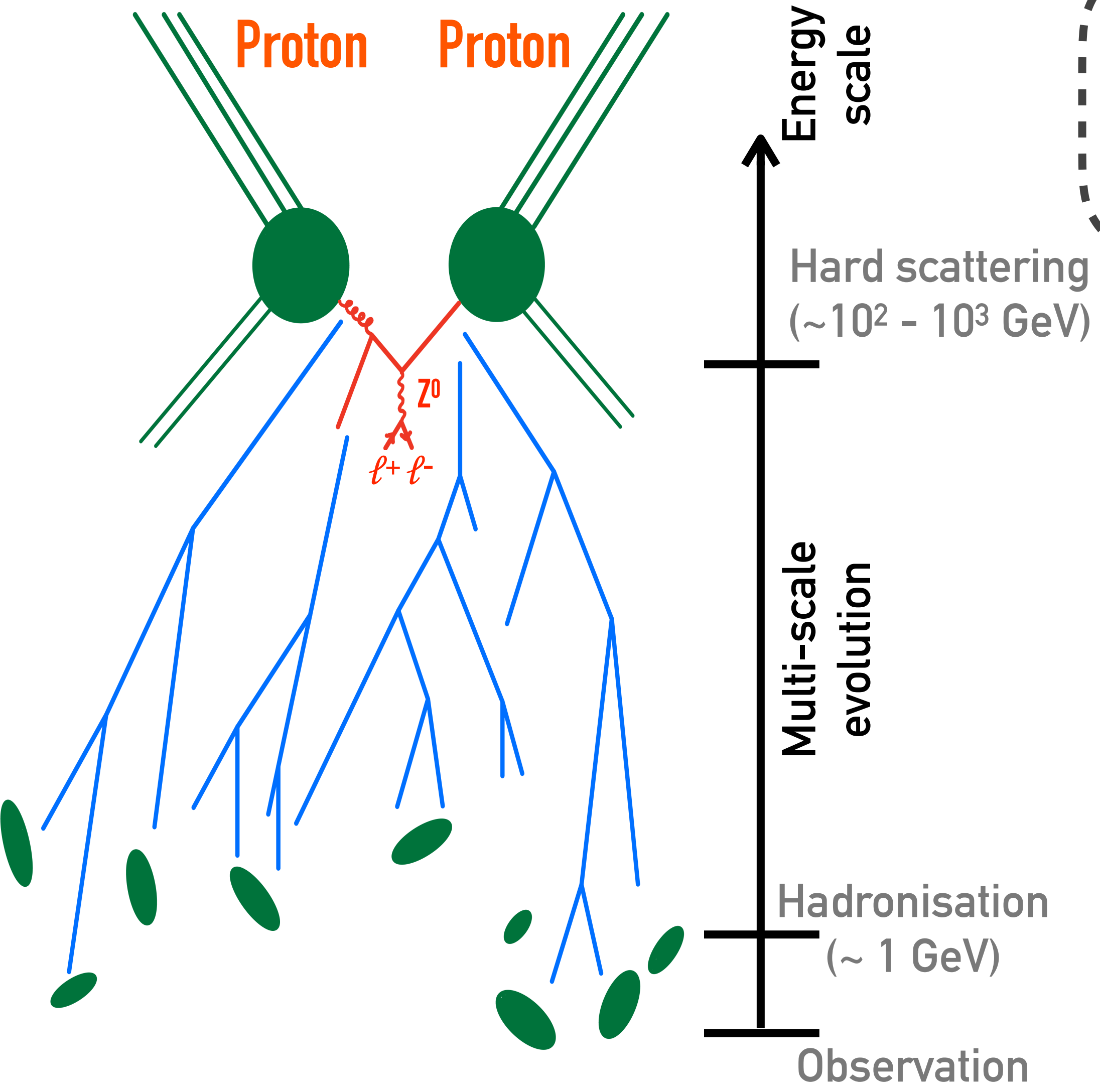
A simplified structure of a LHC event



A simplified structure of a LHC event



A "spherical-cow" approximation (which however captures most of the physics!)

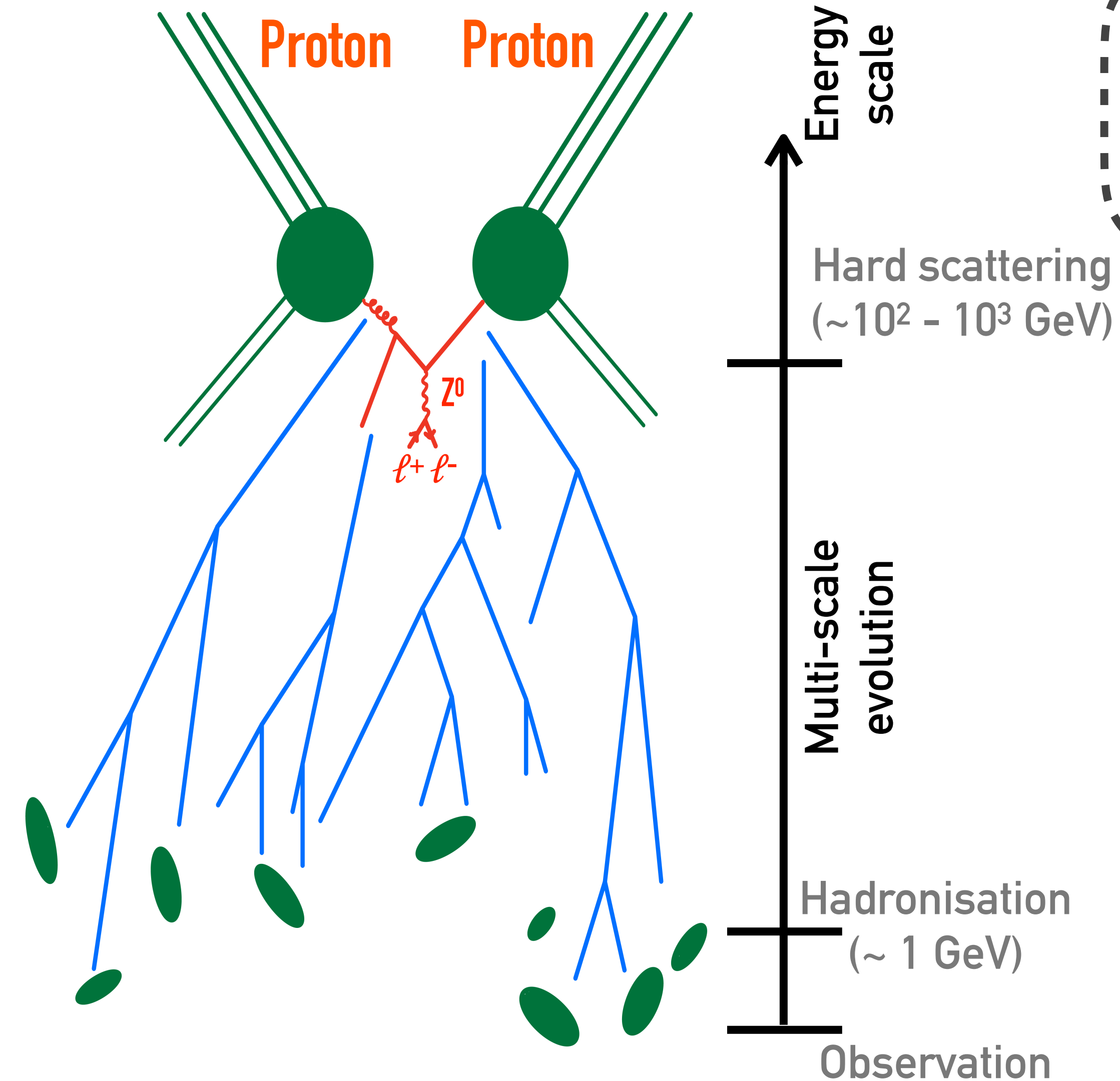


A simplified structure of a LHC event



A “spherical-cow” approximation (which however captures most of the physics!)

- Hard scattering (2 hardest partons): large momentum transfer, where new physics may be hiding
- Multi-scale evol.ⁿ: copious emission of (mainly) strongly interacting particles. System evolves towards lower energies
 - Connects observation/measurement to hard event
- QCD phase transition (non-perturbative): partons are combined into the colour-singlet hadrons eventually observed in the detector

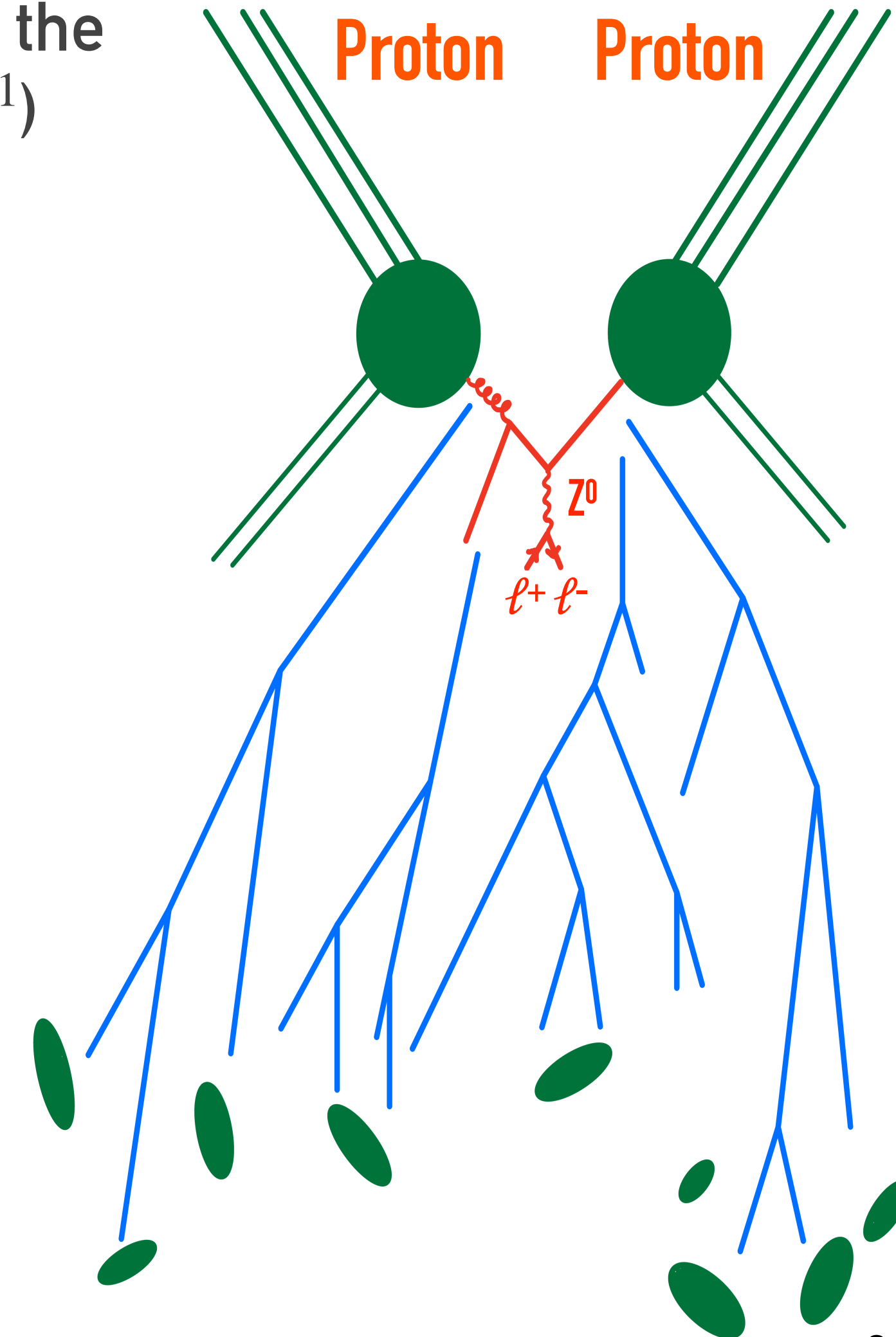


Asymptotic freedom \oplus factorisation \rightarrow perturbative QCD

- Key observation 1: separation (**factorisation**) of dynamics taking place at different time scales \ddagger
 - The “hard” scattering happens on shorter time scales ($\tau \sim 10^{-2} \text{ GeV}^{-1}$) than the interactions within the proton or among the final-state hadrons ($\tau \sim 1 \text{ GeV}^{-1}$)

$$d\sigma_{pp \rightarrow X} = \sum_{ij} \int_0^1 dx_1 dx_2 f_i(x_1, \mu_F) f_j(x_2, \mu_F) \times d\hat{\sigma}_{ij \rightarrow X}(x_1 x_2 S, \mu_R, \mu_F) + \mathcal{O}\left(\frac{\Lambda^p}{m_X^p}\right)$$

Dynamics at **long** time scales
Dynamics at **short** time scales

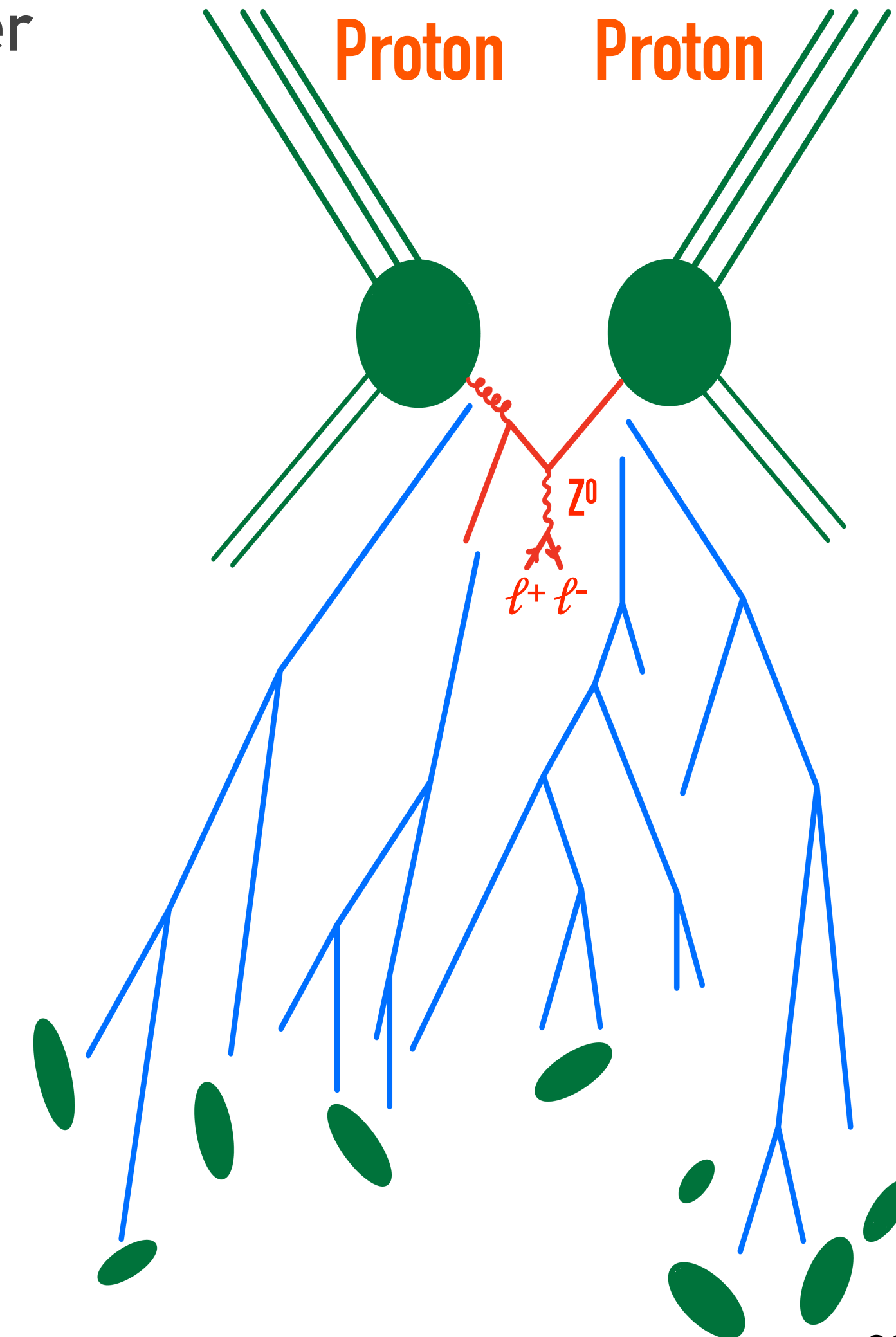


\ddagger Actually proven to all order only for very simple quantities, e.g. Drell-Yan total cross section

Asymptotic freedom \oplus factorisation \rightarrow perturbative QCD

- Key observation 2: strong interactions become weakly coupled at high energies (**asymptotic freedom**)
- Allows for a perturbative approximation of the primary scattering as a power series in α_s (truncated when the desired precision is reached)

$$d\sigma_{pp \rightarrow X} = \sum_{ij} \int_0^1 dx_1 dx_2 f_i(x_1, \mu_F) f_j(x_2, \mu_F) \times \underbrace{d\hat{\sigma}_{ij \rightarrow X}(x_1 x_2 S, \mu_R, \mu_F)}_{\sum_n \alpha_s^{n+n_B}(\mu_R) d\hat{\sigma}_{ij \rightarrow X}^{(n)}} + \mathcal{O}\left(\frac{\Lambda^p}{m_X^p}\right)$$



Asymptotic freedom \oplus factorisation \rightarrow perturbative QCD

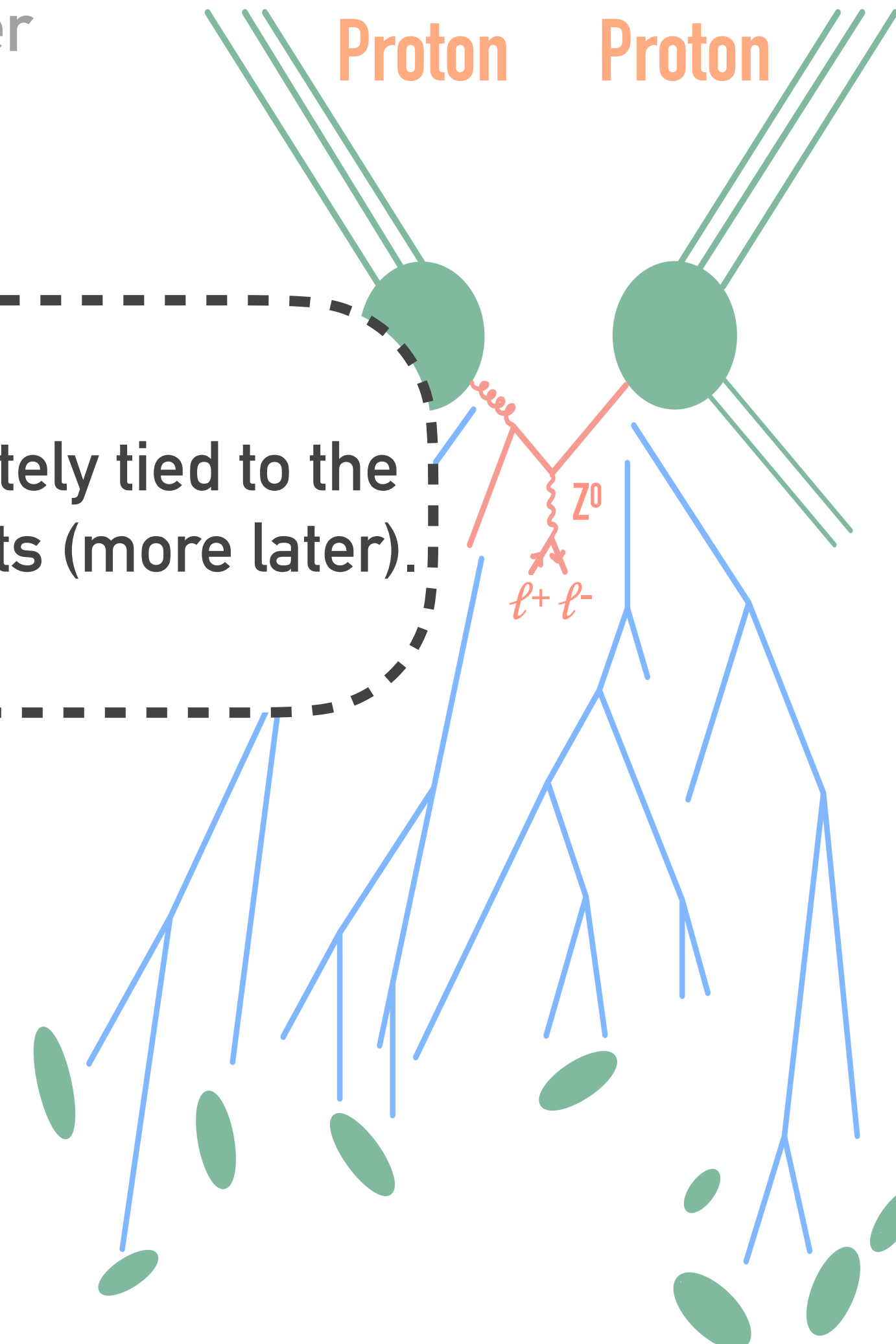
- Key observation 2: strong interactions become weakly coupled at high energies (**asymptotic freedom**)
- Allows for a perturbative approximation of the primary scattering as a power series in α_s (truncated when the desired precision is reached)

$d\sigma_{pp \rightarrow X}$

The properties of **asymptotic freedom** and **factorisation** are intimately tied to the **divergences** structure of gauge theories in different kinematic limits (more later).

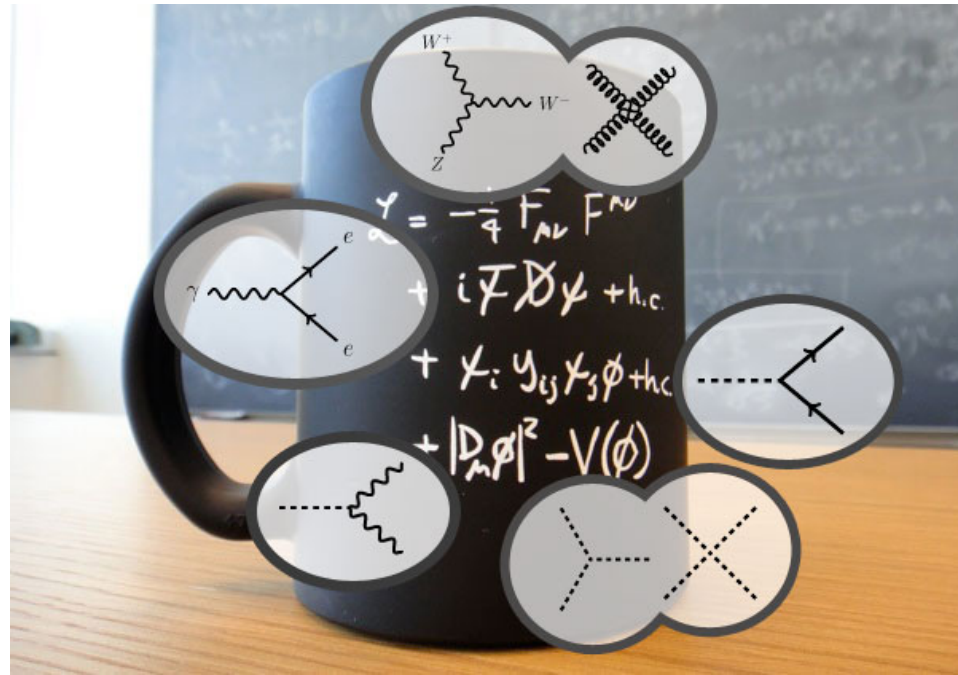
$$\times d\sigma_{ij \rightarrow X}(x_1 x_2 S, \mu_R, \mu_F) + \mathcal{O}\left(\frac{1}{m_X^p}\right)$$

$$\sum_n \alpha_s^{n+n_B}(\mu_R) d\hat{\sigma}_{ij \rightarrow X}^{(n)}$$

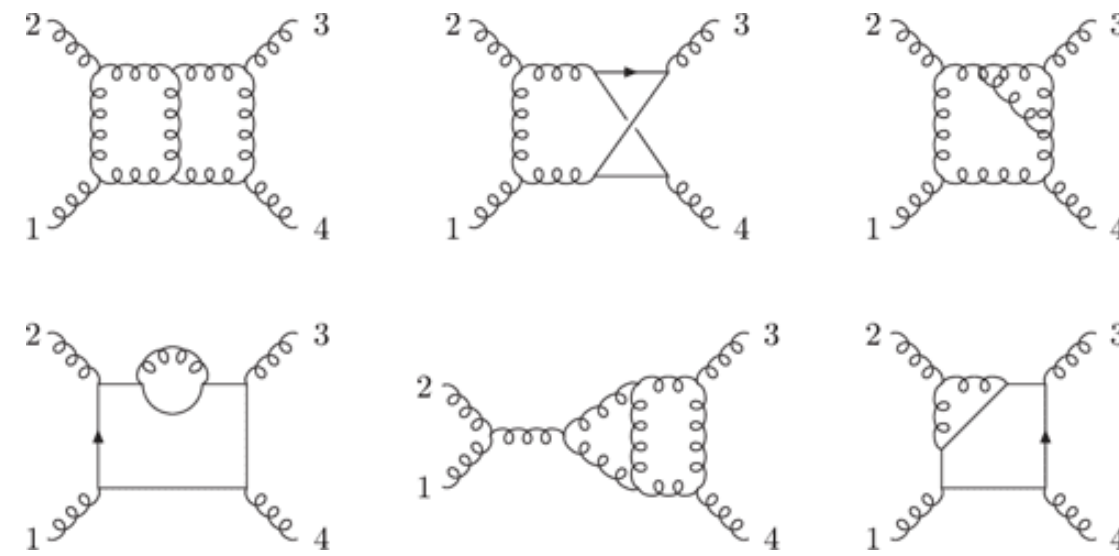


The perturbative-QCDer's workflow

Feynman rules



Scattering amplitudes



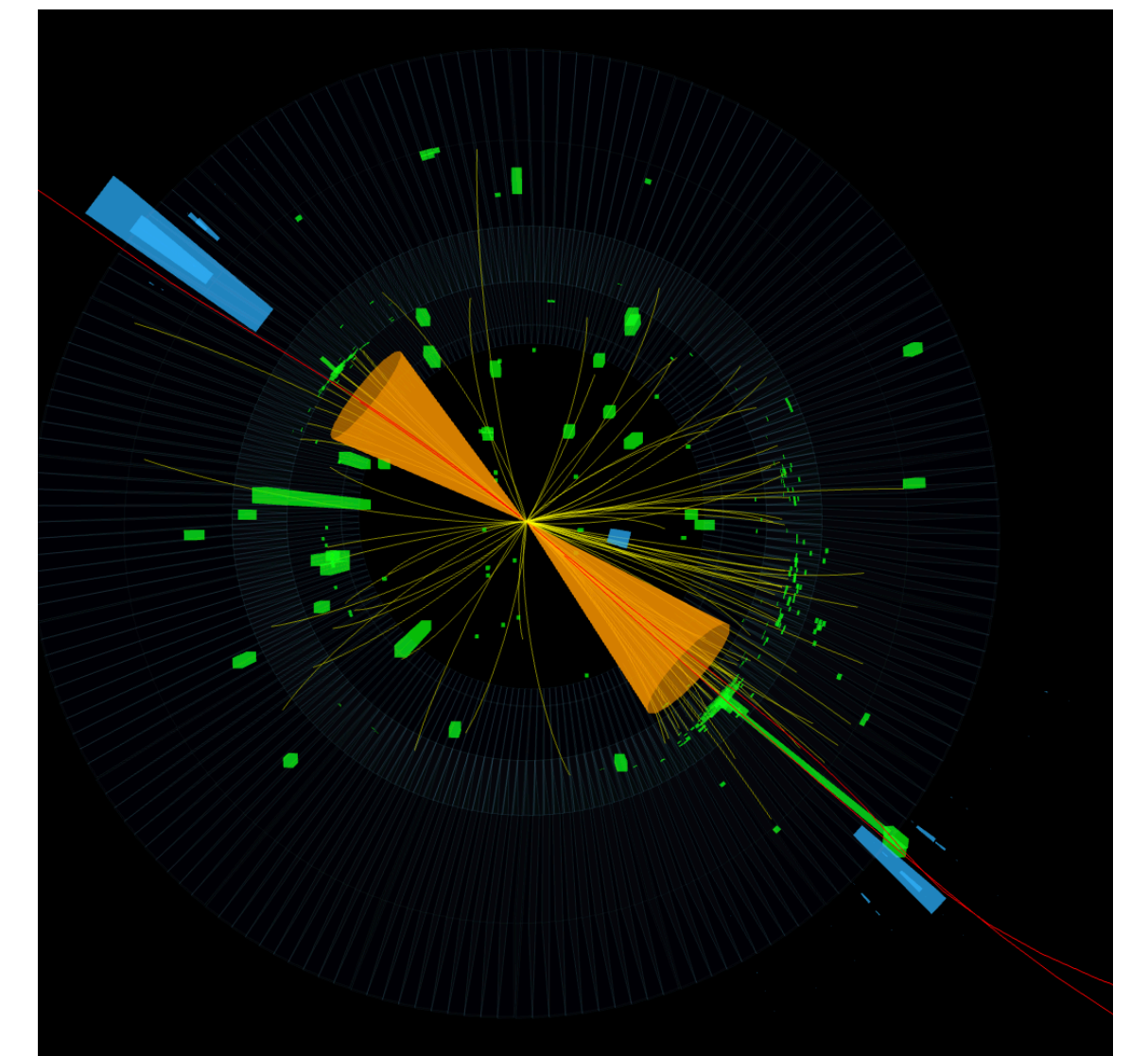
Cross sections

$$d\hat{\sigma}_{2\rightarrow n} = \frac{1}{F} \int \langle |\mathcal{A}|^2 \rangle d\Phi_n \mathcal{O}(\Phi_n)$$

$$d\sigma_{2\rightarrow n} = \int f_1(x_1) f_2(x_2) d\hat{\sigma} dx_1 dx_2$$

Event rates

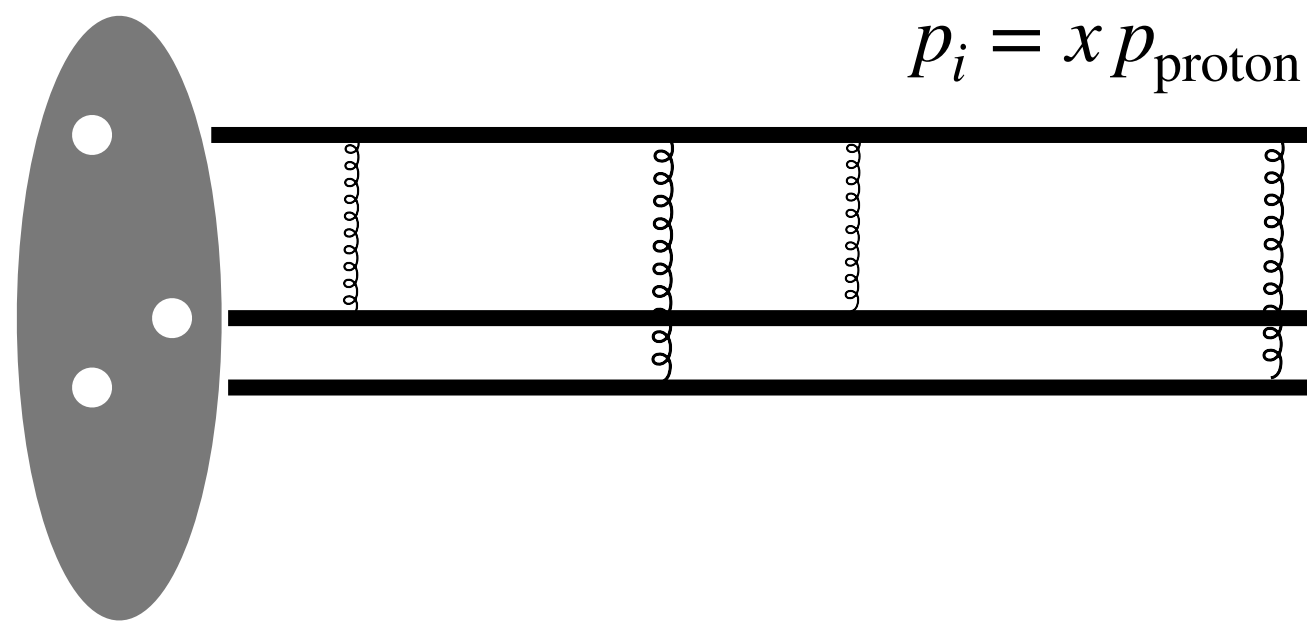
$$N_{\text{events}} = \mathcal{L} \times \sigma$$



Ingredients of the master formula: parton distribution functions

- PDF $f_i(x, \mu)$ encodes the distribution of partons of flavour i and longitudinal momentum x within the proton probed at a scale μ . Composition of the proton evolves with the scale μ (QCD improved parton model).
- Heuristic interpretation in factorisation theorem: resolve partons in the proton at resolution scale μ_F

$$d\sigma_{pp \rightarrow X} = \sum_{ij} \int_0^1 dx_1 dx_2 f_i(x_1, \mu_F) f_j(x_2, \mu_F) \times d\hat{\sigma}_{ij \rightarrow X}(x_1 x_2 s, \mu_R, \mu_F) + \mathcal{O}\left(\frac{\Lambda^P}{m_X^P}\right)$$



In collinear factorisation partons fly in exactly the same direction as the proton, and share its longitudinal momentum. Transverse d.o.f.s are neglected as part of Λ^P / m_X^P corrections (higher twist).

DGLAP evolution equation

- Key property: although PDFs are intrinsically non-perturbative objects, their evolution with the scale at which the proton is resolved is perturbative! The evolution is governed by the **DGLAP equation**

The scale evolution of a flavour interplays with that of other flavours via the anomalous dimension \hat{P}_{ij}

$$\frac{d}{d \ln \mu^2} f_i(x, \mu) = \frac{\alpha_s(\mu)}{2\pi} \int_x^1 \frac{dz}{z} \hat{P}_{ij}(z, \alpha_s(\mu)) f_j\left(\frac{x}{z}, \mu\right) \equiv \frac{\alpha_s(\mu)}{2\pi} \hat{P}_{ij}(x, \alpha_s(\mu)) \otimes f_j(x, \mu)$$

Splitting functions

$$\hat{P}_{ij}(z, \alpha_s(\mu)) = \hat{P}_{ij}^{(0)}(z) + \frac{\alpha_s(\mu)}{2\pi} \hat{P}_{ij}^{(1)}(z) + \mathcal{O}(\alpha_s^2)$$

$$\hat{P}_{qq}^{(0)}(z) = C_F \left(\frac{1+z^2}{(1-z)_+} + \frac{3}{2} \delta(1-z) \right), \quad b_0 = \frac{11C_A - 4T_R n_f}{6}$$

$$\hat{P}_{gg}^{(0)}(z) = 2C_A \left(\frac{z}{(1-z)_+} + \frac{1-z}{z} + z(1-z) \right) + \delta(1-z)b_0$$

$$\hat{P}_{gq}^{(0)}(z) = T_R(z^2 + (1-z)^2), \quad \hat{P}_{qg}^{(0)}(z) = C_F \frac{1+(1-z)^2}{z}$$

“Plus” distributions regularise the soft singularities due to the radiation of a gluon ($z \rightarrow 1$). Notice the enhancement at $z \rightarrow 0$, which drives the growth of the gluon PDF with the scale μ in this regime.

Currently, the complete NNLO splitting functions ($\hat{P}^{(2)}(z)$), and many of the N³L0 terms ($\hat{P}^{(3)}(z)$) are known.

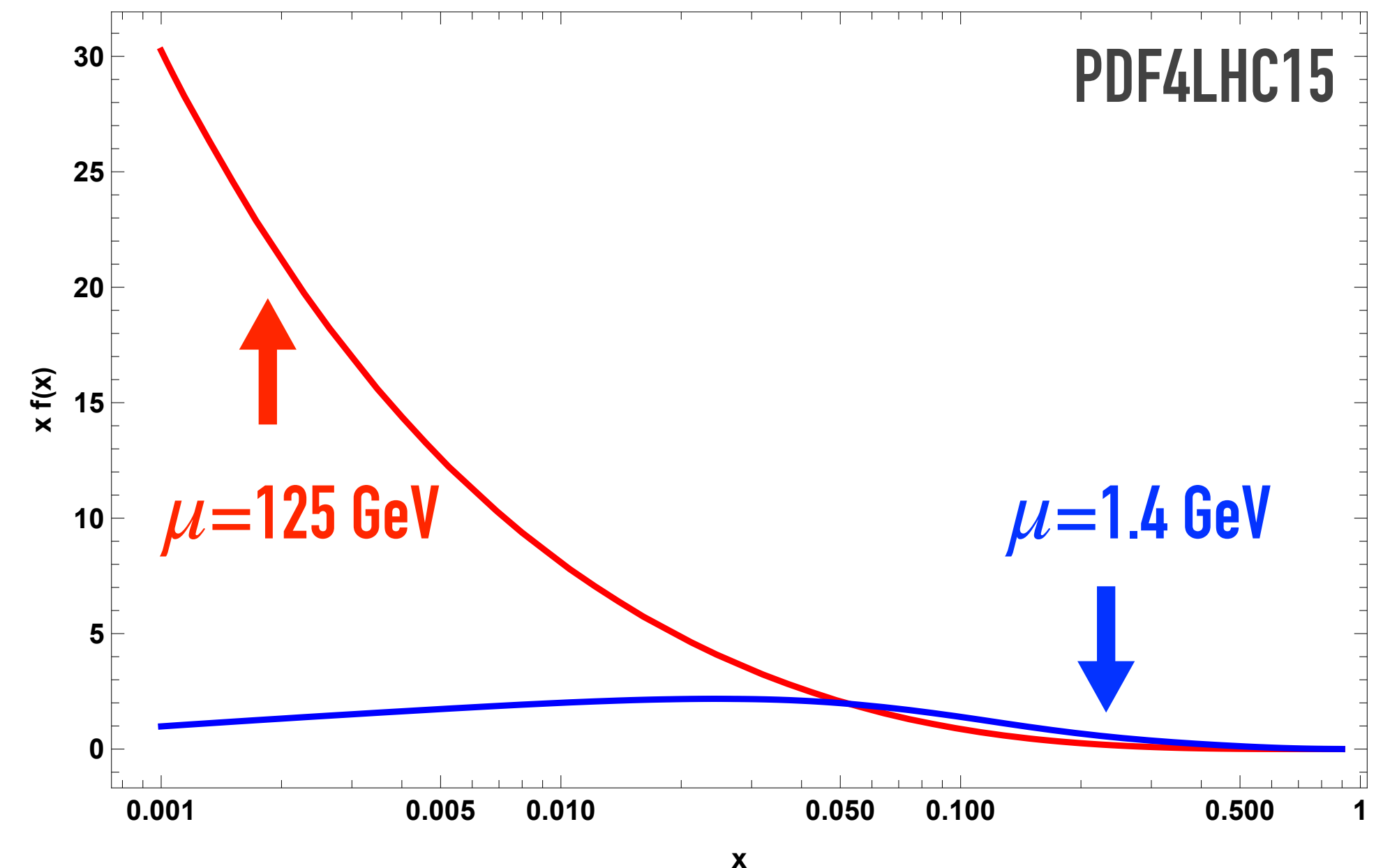
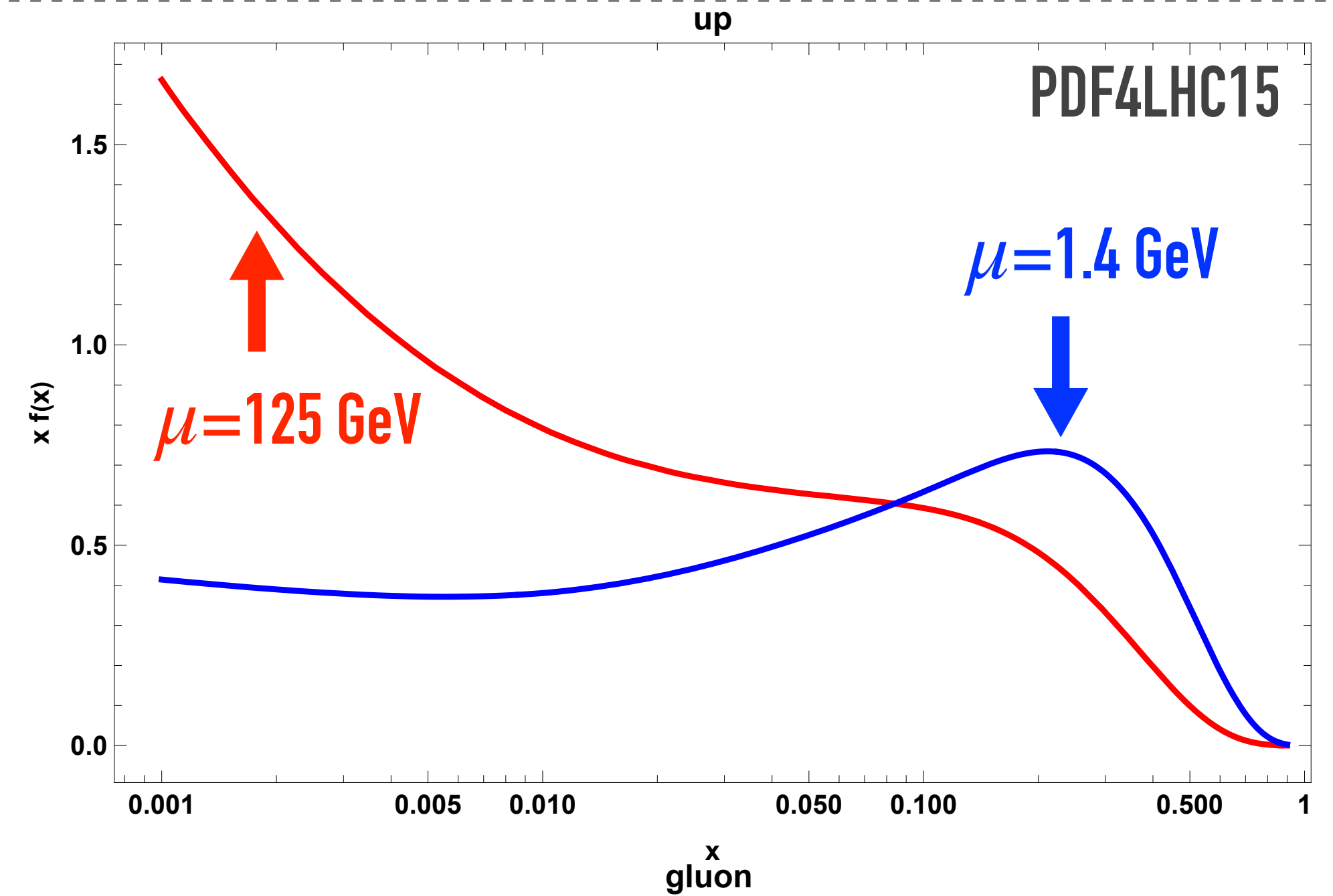
DGLAP evolution equation

Figures made with [ManeParse](#) public code (see also [Apfel](#))

Mathematica code available at this [URL](#)

DGLAP evolution towards larger scales depletes the distributions at larger x to fuel the growth of the distributions at smaller x .

Gluon PDF becomes substantial. Its growth is driven by $q \rightarrow qg$ and $g \rightarrow gg$ splittings (enhancement of corresponding splitting functions)



Composition of the proton

Figures made with [ManeParse](#) public code (see also [Apfel](#))

DGLAP evolution determines the composition of the proton at perturbative scales given a fit of the parton densities at small (\sim non-perturbative) scales.

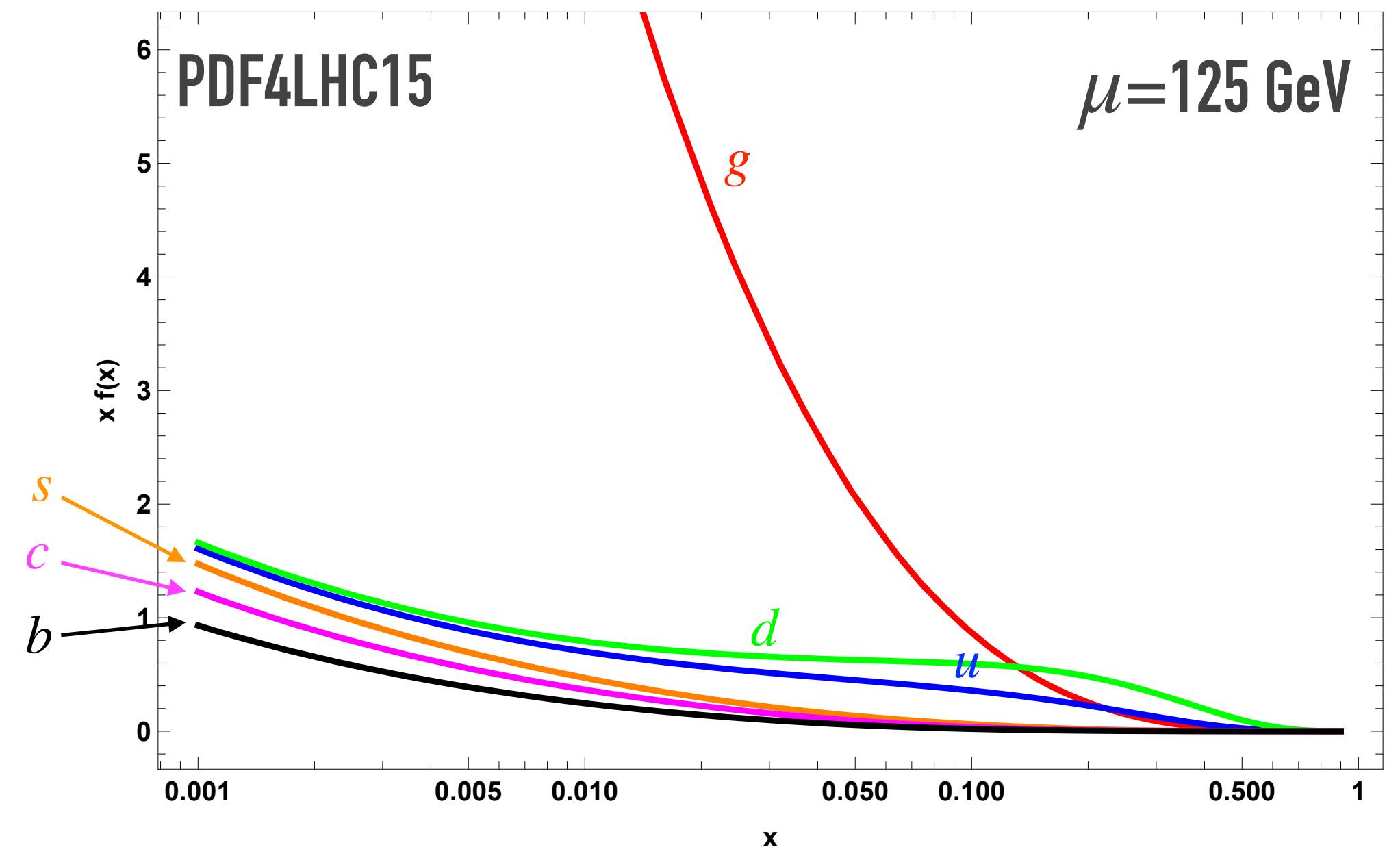
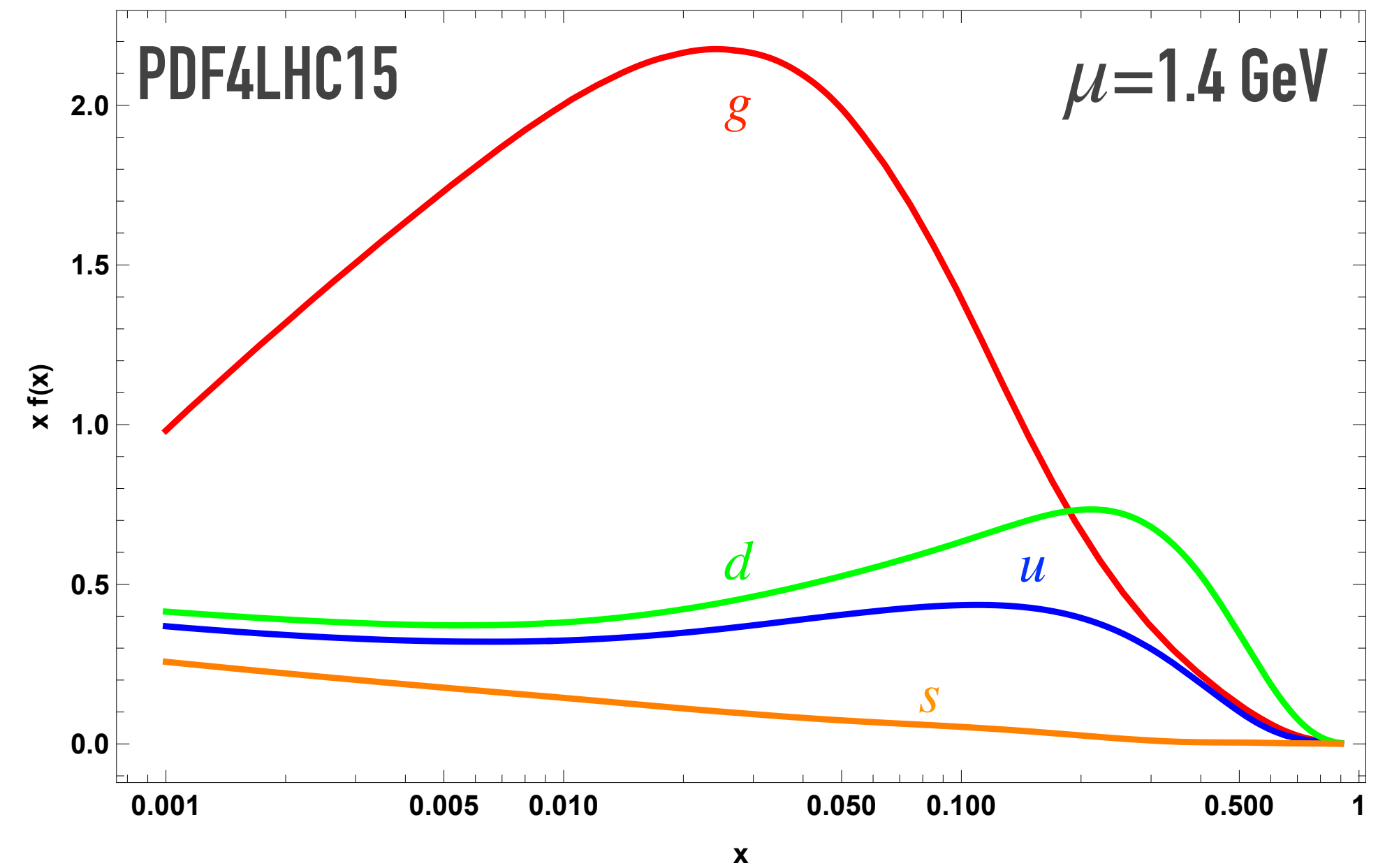
The growth of the gluon PDFs has a substantial impact on LHC phenomenology (e.g. Higgs, $t\bar{t}$, jets,...).

Heavier flavours (e.g. c, b) are produced dynamically via gluon splitting. Ongoing debate as to whether there is an “intrinsic” component in the proton (e.g. intrinsic charm)

Momentum sum rule:

$$\int_0^1 dx x \left(\sum_{i \in q, \bar{q}} f_i(x, \mu) + f_g(x, \mu) \right) = 1$$

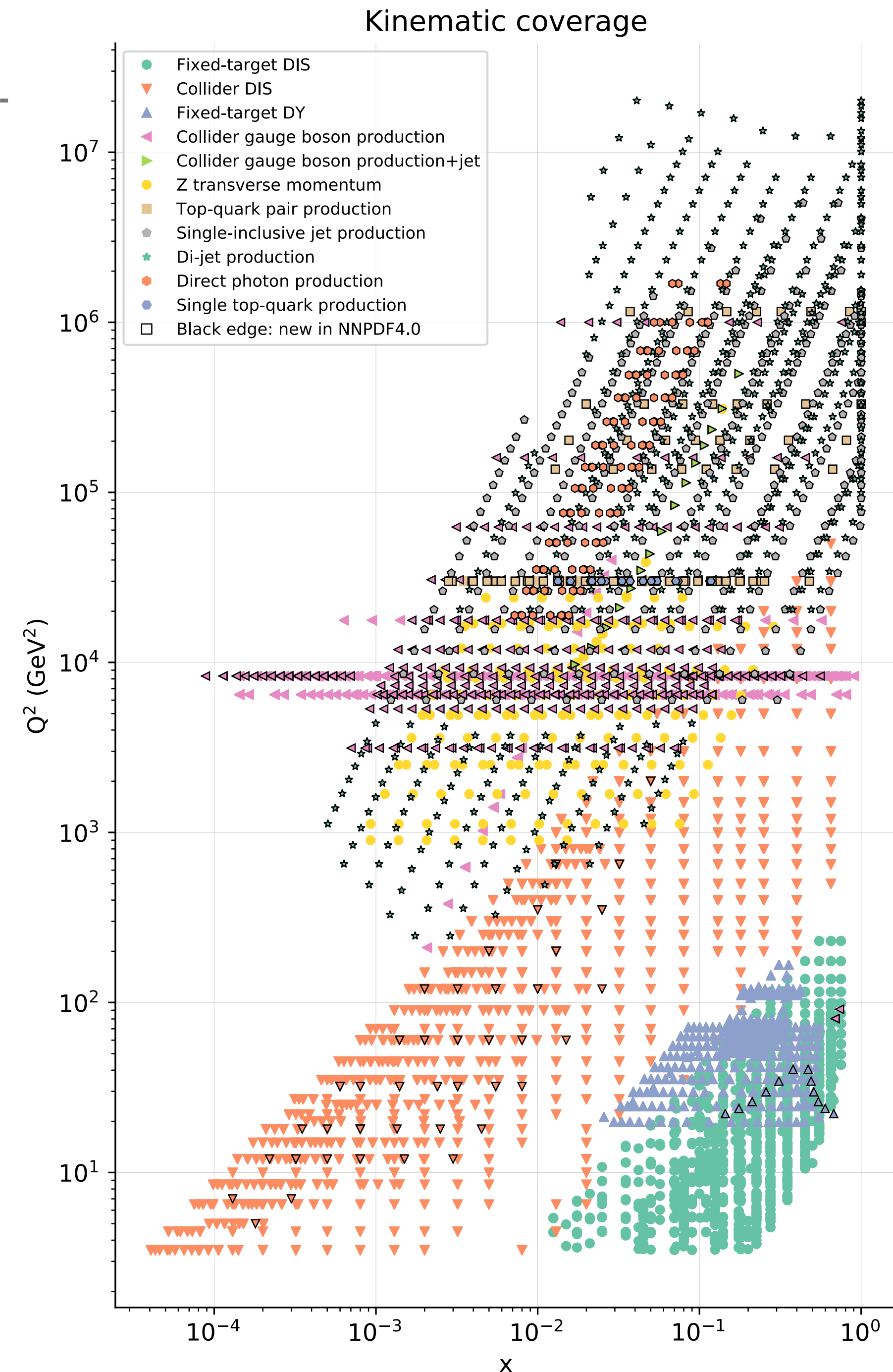
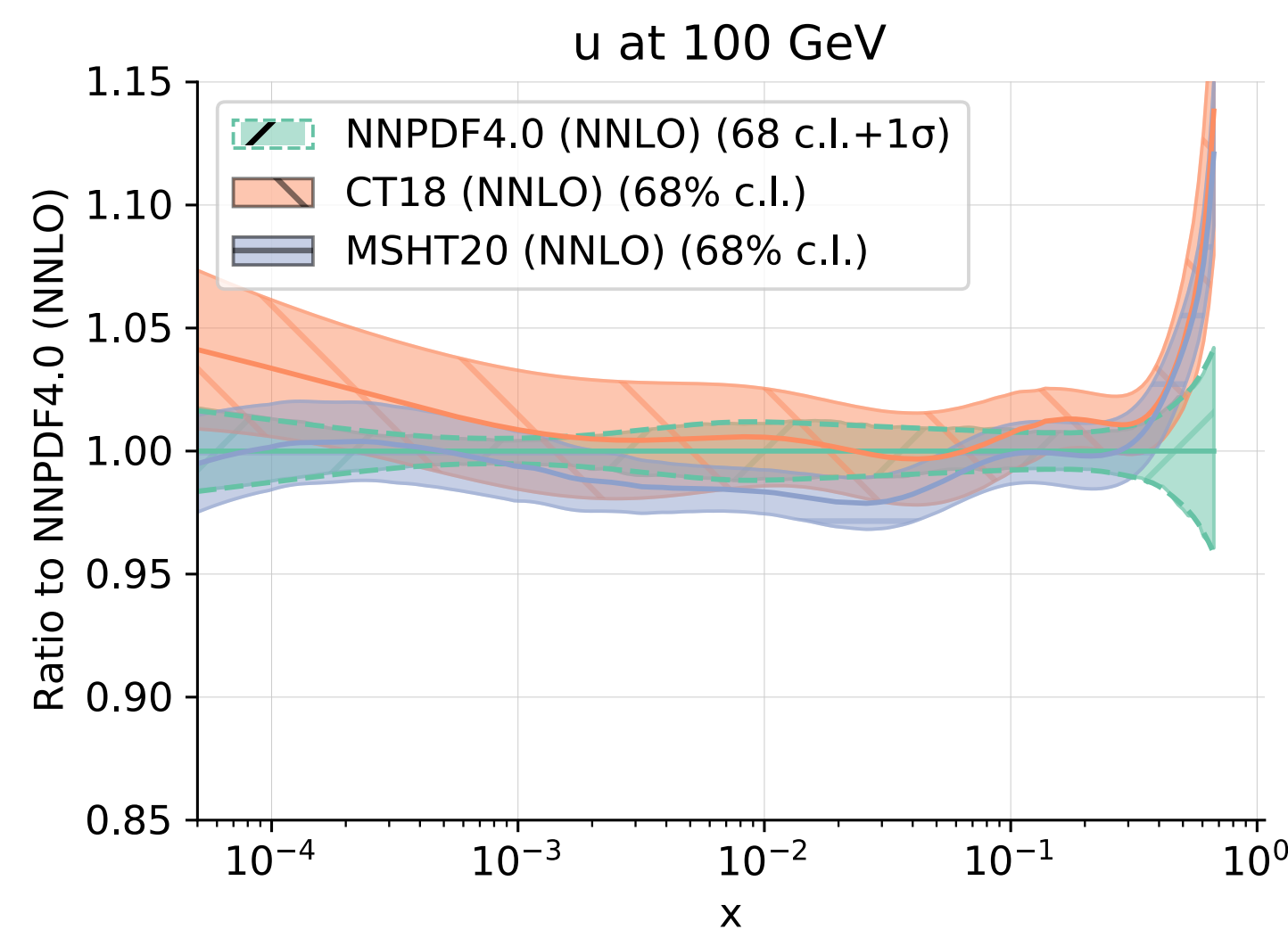
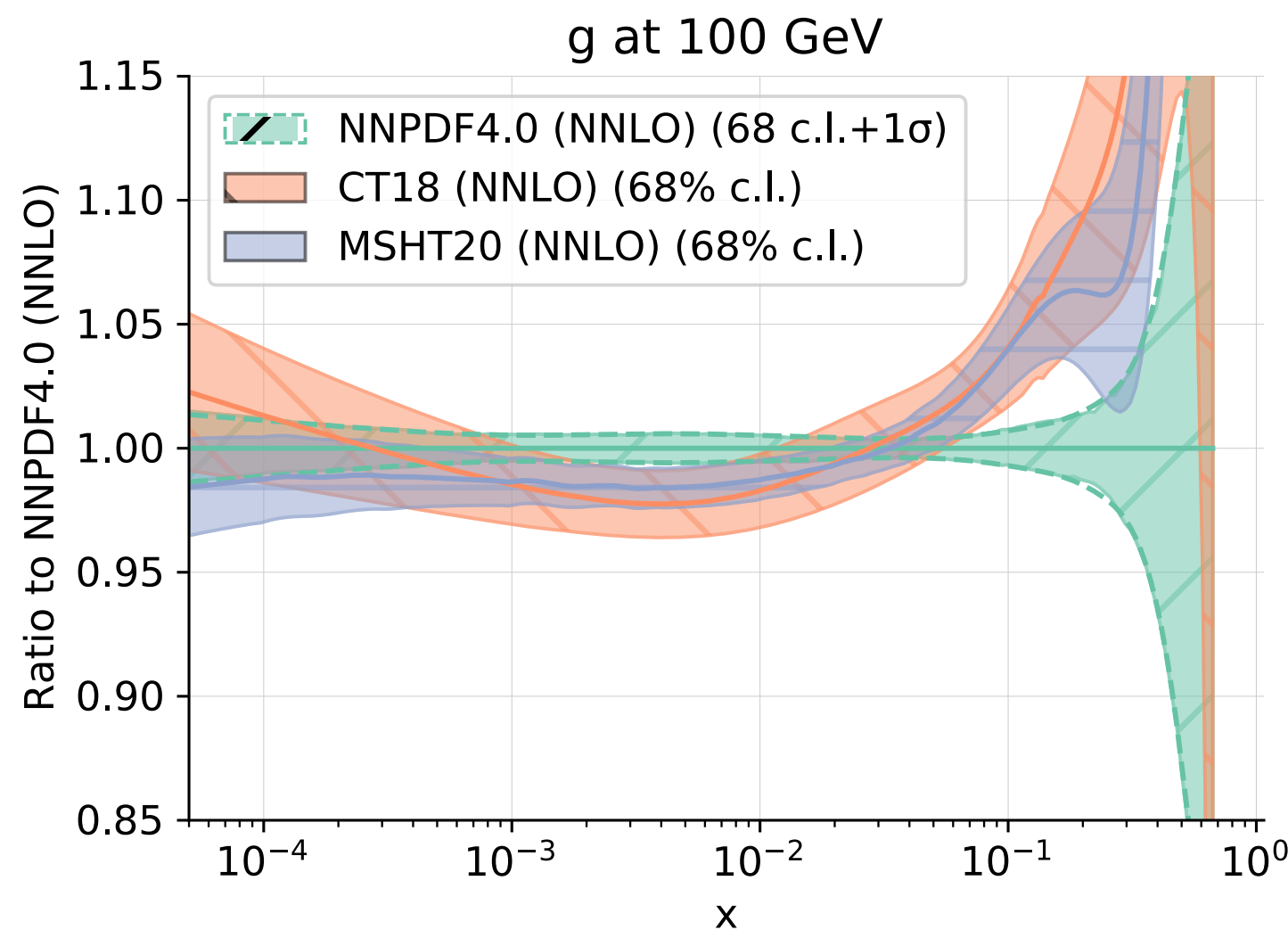
Gluons carry roughly 50% of the proton's momentum at $\mu = m_h$



Current status of global PDF determinations

- Many determinations for LHC. Modern global fits reach few-% precision for $x \in [10^{-3}, 0.1]$, although estimate of PDF uncertainties is currently an open problem (fit/theory uncertainties)
- State of the art sets are extracted with NNLO (DGLAP and QCD predictions for $\hat{\sigma}$), and a lot of data. First steps towards N³L0 sets are being taken

e.g. Comparison of PDFs (g & u) between different fitting methodologies (neural networks, hessian, ...) and parametric settings (m_c, α_s, \dots)



Ingredients of the master formula: the partonic cross section

- Encodes the actual perturbative part of the high-energy partonic scattering

$$d\sigma_{pp \rightarrow X} = \sum_{ij} \int_0^1 dx_1 dx_2 f_i(x_1, \mu_F) f_j(x_2, \mu_F) \times \underbrace{d\hat{\sigma}_{ij \rightarrow X}(x_1 x_2 S, \mu_R, \mu_F)}_{\sum_n \alpha_s^{n+n_B}(\mu_R) d\hat{\sigma}_{ij \rightarrow X}^{(n)}} + \mathcal{O}\left(\frac{\Lambda^p}{m_X^p}\right)$$

$$d\hat{\sigma}_{ij \rightarrow X}(x_1 x_2 S, \mu_R, \mu_F) = \alpha_s^{n_B}(\mu_R) \left(\begin{array}{cccc} \text{LO} & \text{NLO} & \text{NNLO} & \text{N}^3\text{LO} \\ \text{(TH error } \sim 50\%) & \text{(TH error } \sim 20\%) & \text{(TH error } \sim 5-10\%) & \text{(TH error } \sim \text{few } \%) \\ d\hat{\sigma}_{ij \rightarrow X}^{(0)} & + \alpha_s(\mu_R) d\hat{\sigma}_{ij \rightarrow X}^{(1)} & + \alpha_s^2(\mu_R) d\hat{\sigma}_{ij \rightarrow X}^{(2)} & + \alpha_s^3(\mu_R) d\hat{\sigma}_{ij \rightarrow X}^{(3)} + \dots \end{array} \right)$$

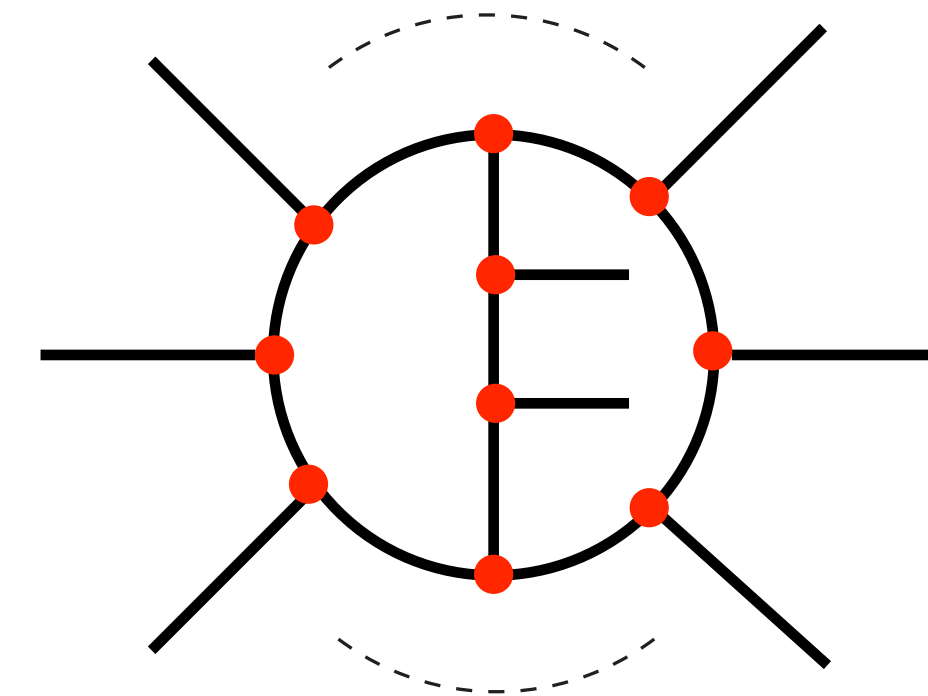
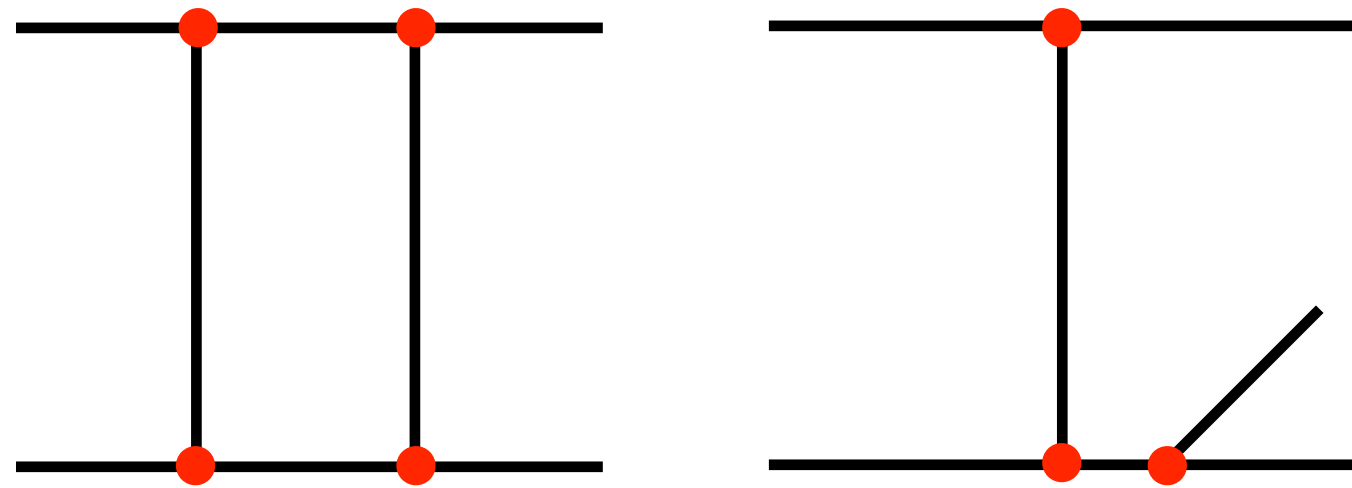
LO (Born) cross section, $n_B > 0$ for QCD mediated processes (e.g. $gg \rightarrow h, t\bar{t}, \text{jets}$)

The dependence on the unphysical scales (μ_R, μ_F) will always be of higher orders w.r.t. the perturbative accuracy reached (gives a handle to estimate the size of missing corrections)

Computing the partonic cross section

$$d\hat{\sigma}_{ij \rightarrow X}^{(n)} = \frac{1}{F} \sum_m \int d\Phi_m \langle |\mathcal{A}_{2 \rightarrow m}|^2 \rangle \mathcal{O}(\Phi_m)$$

Flux factor \bullet $\frac{1}{F}$
 m body phase space (for all m contributing to a given perturbative order)
 $\langle |\mathcal{A}_{2 \rightarrow m}|^2 \rangle$ Squared amplitude (averaged over initial-state spin & colour)
 $\mathcal{O}(\Phi_m)$ Observable's measurement

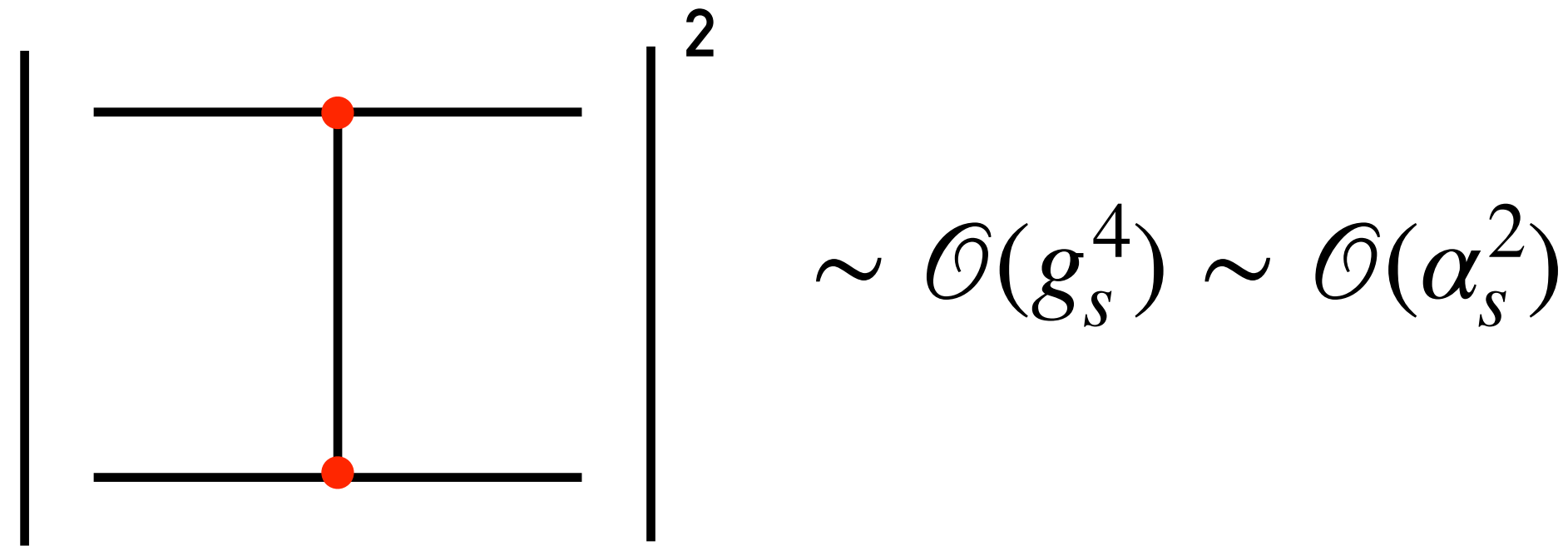


Computation of phase space integrals entails delicate cancellations of singularities (**subtractions**) between real and virtual corrections. Significant computational challenge for state of the art calculations

Computation of scattering amplitudes at higher loops: entails VERY large expressions (algebraic complexity) & spaces of special functions (analytic complexity)

The squared amplitude (e.g. NLO for $2 \rightarrow 2$ partonic process)

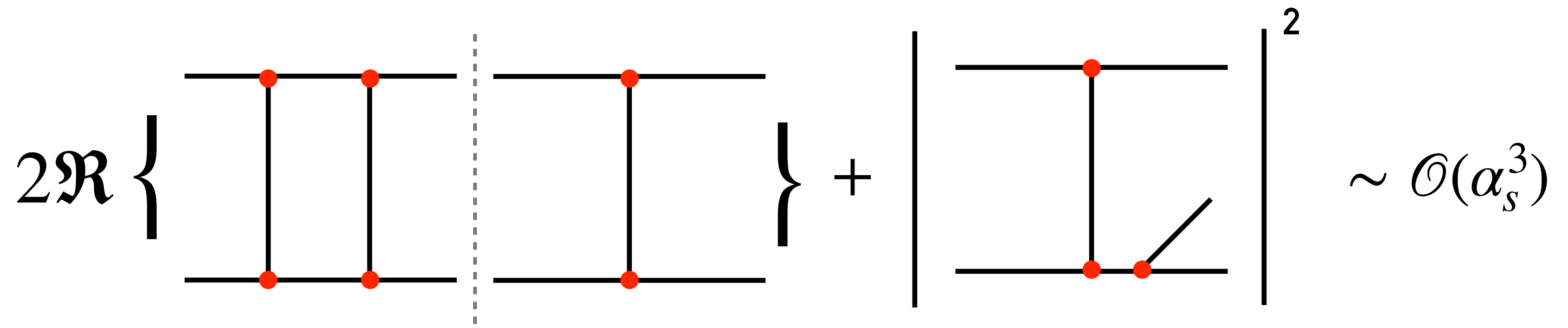
LO‡
(only tree-level diagrams)



NLO‡

1) Add a virtual loop to the LO process and expand the squared norm

2) Add a real emission to the LO process



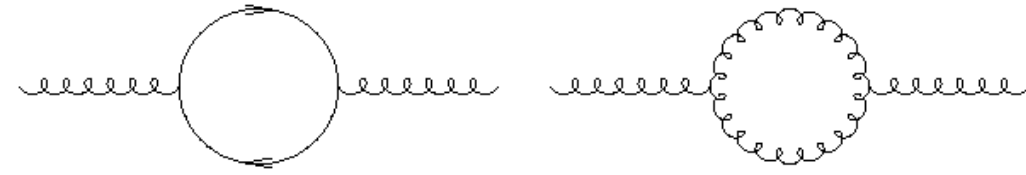
$$|\mathcal{A}^{(0)} + \alpha_s \mathcal{A}^{(1)}|^2 = |\mathcal{A}^{(0)}|^2 + \alpha_s 2\Re \mathcal{A}^{(0)} (\mathcal{A}^{(1)})^\dagger + \dots$$

Which type of diagrams enter a NNLO calculation for this reaction?

‡ We use representative diagrams, the actual number of Feynman diagrams explodes with the perturbative order

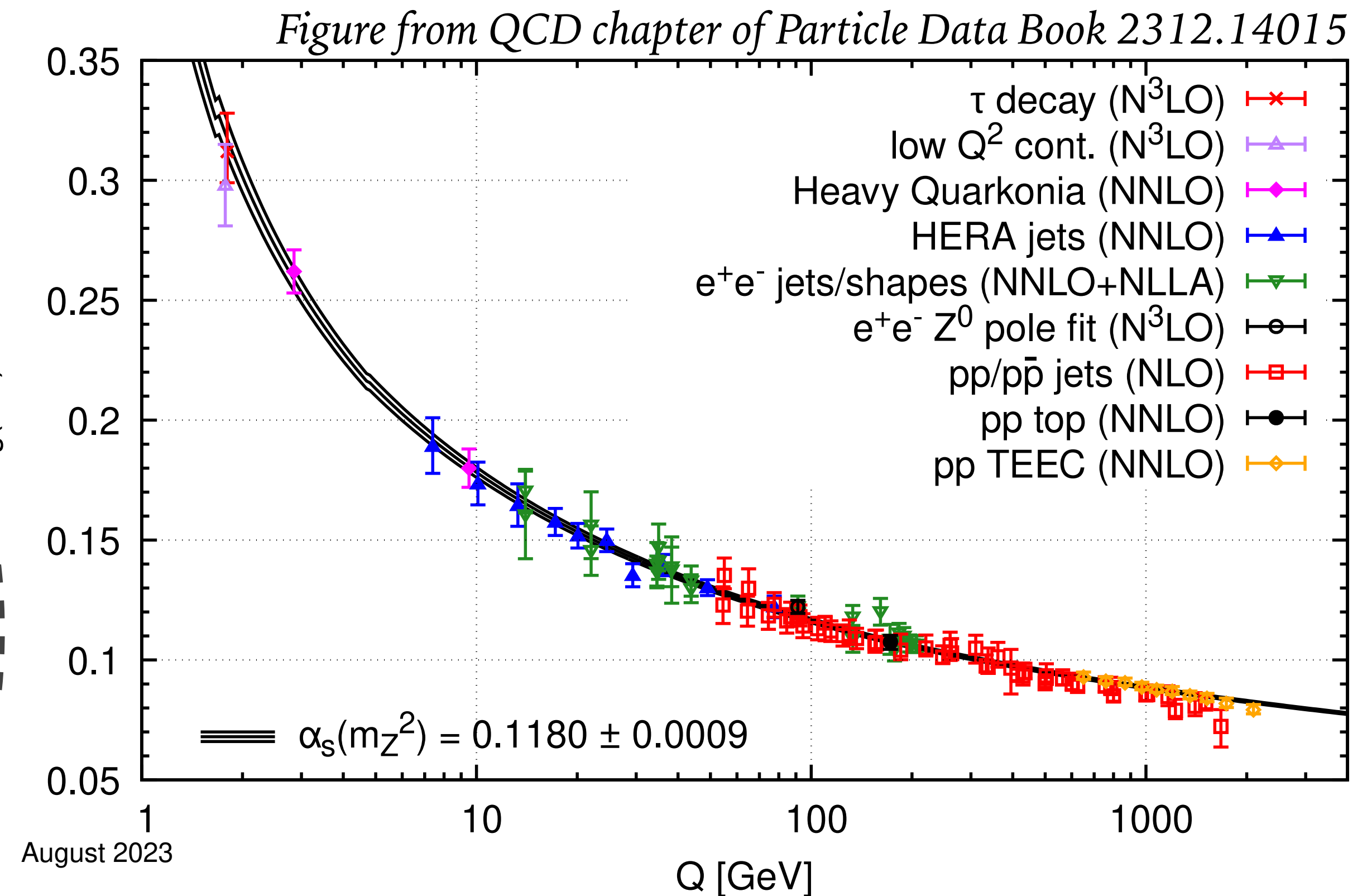
Ingredients of the master formula: the strong coupling constant

- The size of α_s determines how many perturbative orders are needed to reach the desired precision
- As for PDFs, the coupling “runs” with the energy scale (**renormalisation group equation**)

$$\frac{d\alpha_s(\mu)}{d \ln \mu^2} = \beta(\alpha_s(\mu)) \stackrel{\ddagger}{=} -\beta_0 \alpha_s^2(\mu) + \mathcal{O}(\alpha_s^3), \quad \beta_0 = (11C_A - 4T_R n_f)/(12\pi) > 0$$


$$\alpha_s(\mu) = \frac{\alpha_s(\mu_0)}{1 + \alpha_s(\mu_0)\beta_0 \ln \frac{\mu^2}{\mu_0^2}} = \frac{1}{\beta_0 \ln \frac{\mu^2}{\Lambda^2}}$$

Coupling becomes small at large scales (asymptotic freedom) and has a logarithmic divergence at small scales (breakdown of pQCD due to confinement) parametrised by theory IR cutoff Λ



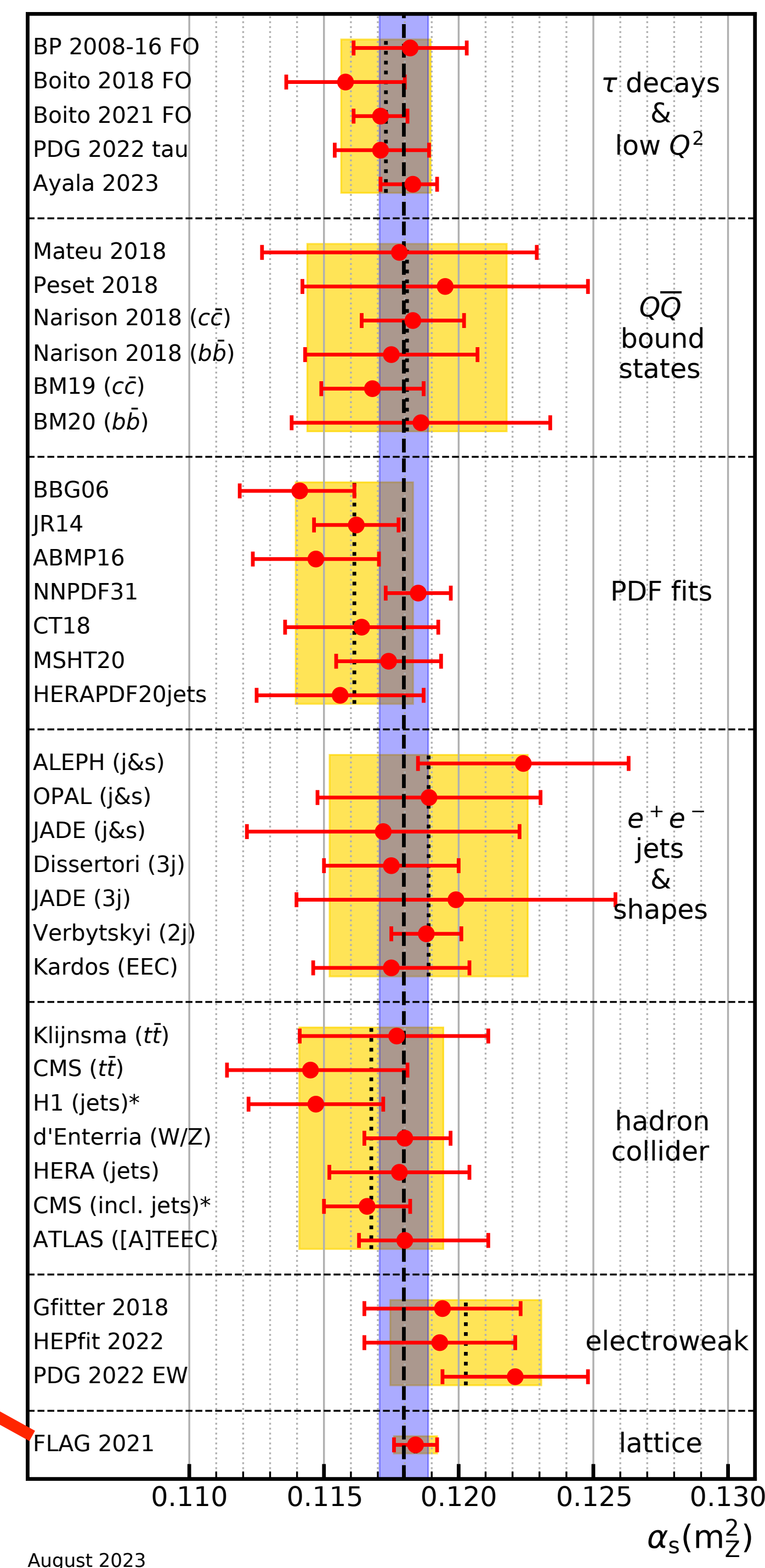
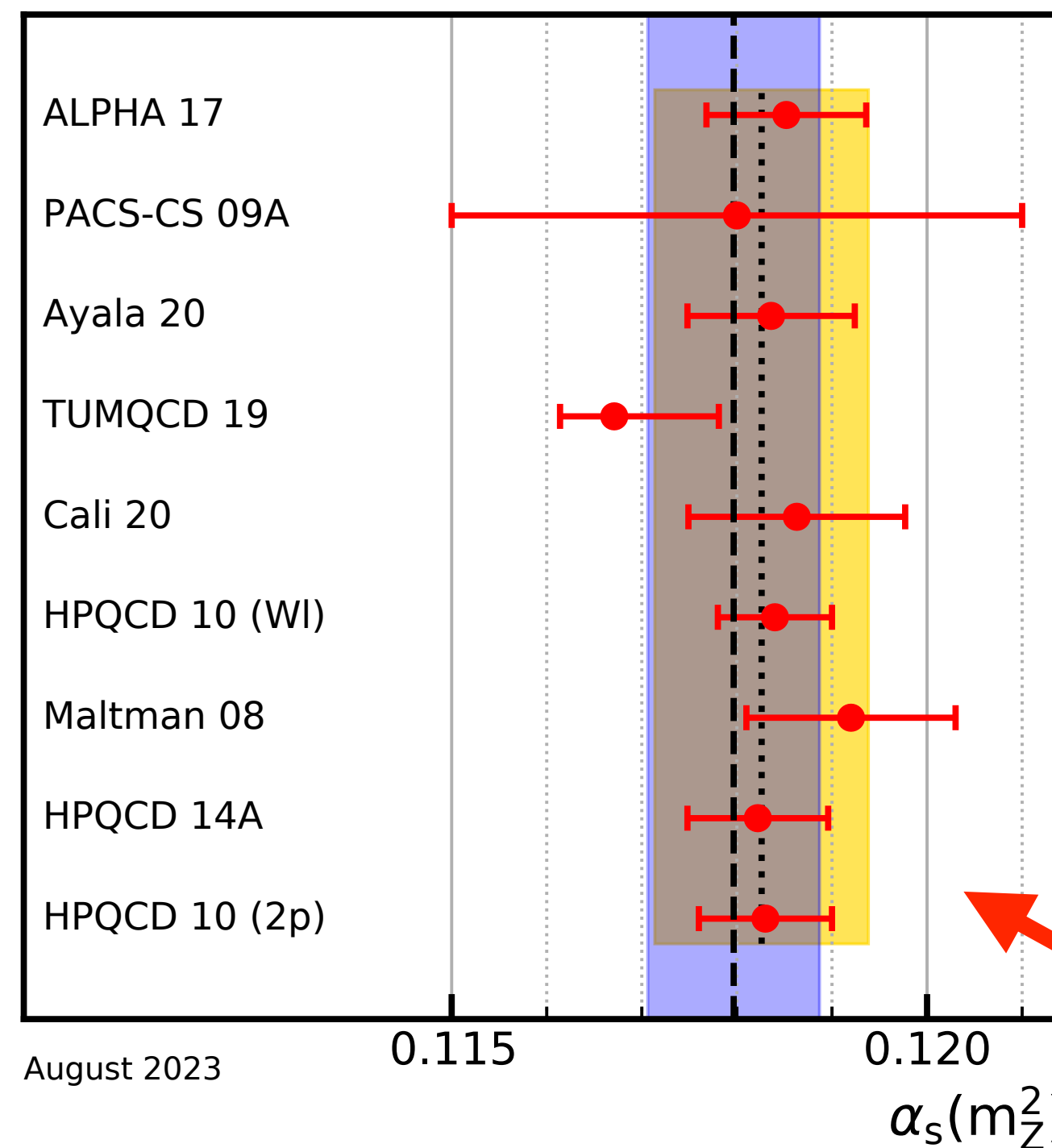
$\ddagger \beta(\alpha_s)$ currently known to 5 loops!

Precise determinations of the strong coupling constant

- As for PDFs, we can predict the evolution between scales but not the absolute value of the coupling, which must be extracted from data
- Several extractions from different experiments/observables/methods
- Ongoing debate about uncertainties in many fits (e.g. hadronization corr^{ns})
- First-principle computation possible with lattice QCD (many observables), uncert. reliably at and below % level
- Optimistic perspective to reach higher accuracy (few permille) from future lattice extractions and future colliders (e.g. FCC-ee)

2023 World Average:

$$\alpha_s(m_Z) = 0.1180 \pm 0.0009 \text{ (0.76\%)}$$



Ingredients of the master formula: power corrections

- Encode physics at hadronic scale due to either hadronization or dynamics within the protons (e.g. intrinsic transverse momentum, multiple parton scatterings). No general first-principle approach to control them at present (analytic methods in simple cases, otherwise Monte Carlo models)

$$d\sigma_{pp \rightarrow X} = \sum_{ij} \int_0^1 dx_1 dx_2 f_i(x_1, \mu_F) f_j(x_2, \mu_F) \times d\hat{\sigma}_{ij \rightarrow X}(x_1 x_2 S, \mu_R, \mu_F) + \mathcal{O}\left(\frac{\Lambda^p}{m_X^p}\right)$$

→ Value of parameter p is observable dependent & it is crucial for precision physics programme

e.g. if $m_X \sim 100$ GeV a very rough estimate suggests

$$\frac{\Lambda}{m_X} \sim \mathcal{O}(1\%), \quad \left(\frac{\Lambda}{m_X}\right)^2 \sim \mathcal{O}(0.1\%)$$

Some examples: $p=2$ for the Drell-Yan (Higgs) total cross section and related inclusive q_T distribution 😊;
 $p=1$ for most jet observables 😞

**Let's put all this into practice:
The Higgs total cross section (ggF)**

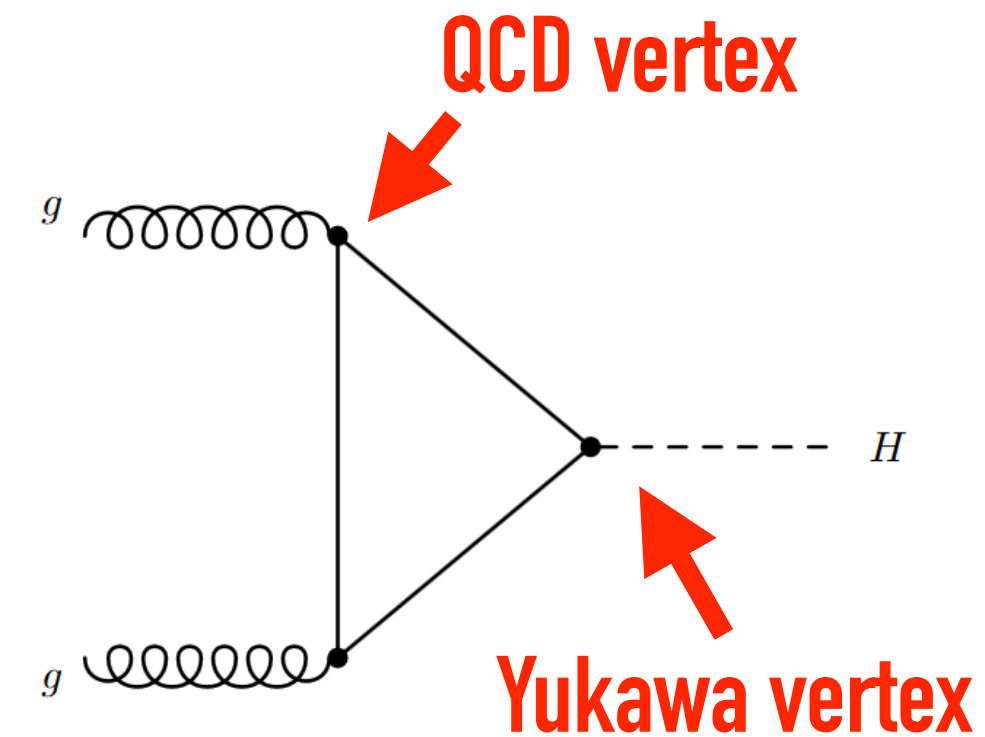
The leading order (LO) cross section (effectively a one loop calculation)

- After averaging over colour & spin states, the partonic XS reads $\hat{\sigma}_0 = A_{gg} \delta(1 - z)$

$$A_{gg} = \frac{\alpha_s(\mu_R)^2}{\pi} \frac{1}{256v^2} \left| \sum_{q \in \text{loop}} \tau_q (1 + (1 - \tau_q) f(\tau_q)) \right|^2, \quad z = \frac{m_h^2}{\hat{s}}$$

$$f(\tau_q) = -\frac{1}{4} \left(\ln \frac{1 + \sqrt{1 - \tau_q}}{1 - \sqrt{1 - \tau_q}} - i\pi \right)^2 \quad \text{if } \tau_q < 1$$

$$f(\tau_q) = \arcsin^2 \left(\sqrt{1/\tau_q} \right) \quad \text{if } \tau_q \geq 1$$



$$\tau_q = 4m_q^2/m_h^2$$

- Total cross section is simply given by

$$\sigma_0 = \int_0^1 dx_1 dx_2 f_g(x_2, \mu_F) f_g(x_1, \mu_F) m_h^2 A_{gg} \delta(\hat{s} - m_h^2) = m_h^2 A_{gg} \mathcal{L}_{gg} \left(\frac{m_h^2}{s} \right) \quad \mathcal{L}_{ij}(\tau) = \int_\tau^1 \frac{dx}{x} f_i(x, \mu_F) f_j \left(\frac{\tau}{x}, \mu_F \right)$$

$$\hat{s} = x_1 x_2 s$$

Parton (gluon)
luminosity

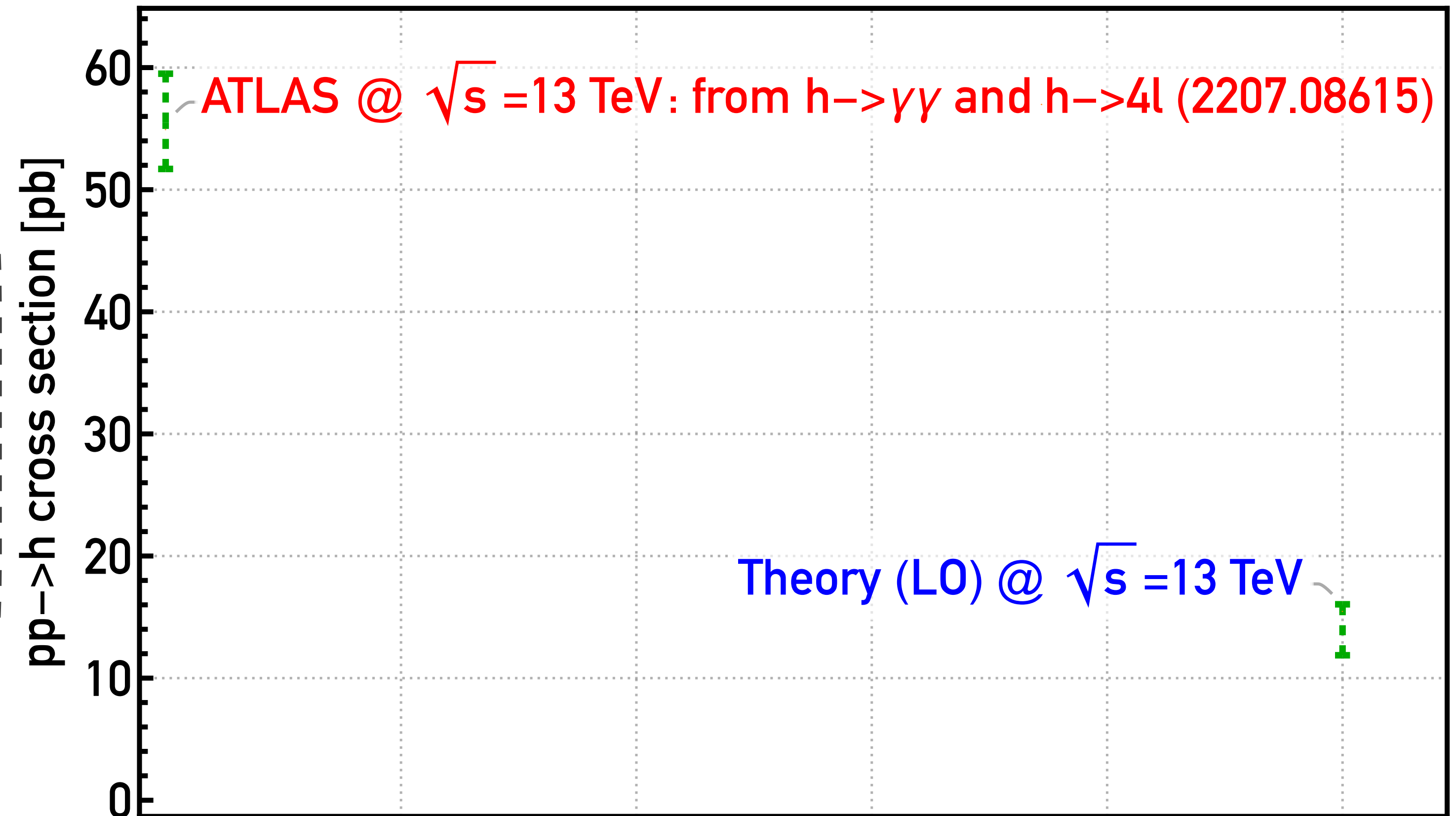
The LO cross section vs. experiment

Predictions here obtained with the [ggHiggs](#) public code

- However, comparison to data reveals a large discrepancy. Possible explanations:
 - It may be a sign of new physics!
 - Is the theory prediction sufficiently accurate & reliable? What is the theory uncertainty of our calculation?

Central obstacle in modern collider physics: getting theoretical calculations to be sufficiently accurate & reliable (e.g. in our case it involves quantum corrections to $gg \rightarrow h$ & other production modes).

Let's consider next-to-leading-order (NLO) corrections next ...



Appendix

The generators of the SU(3) (colour) algebra

- The (traceless and Hermitian) Gell-Mann matrices span the SU(3) Lie algebra $[t^a, t^b] = if^{abc}t^c$, with $t_{ij}^a = \frac{\lambda_{ij}^a}{2}$

$$\lambda^1 = \begin{pmatrix} 0 & 1 & 0 \\ 1 & 0 & 0 \\ 0 & 0 & 0 \end{pmatrix}$$

$$\lambda^2 = \begin{pmatrix} 0 & -i & 0 \\ i & 0 & 0 \\ 0 & 0 & 0 \end{pmatrix}$$

$$\lambda^3 = \begin{pmatrix} 1 & 0 & 0 \\ 0 & -1 & 0 \\ 0 & 0 & 0 \end{pmatrix}$$

$$\lambda^4 = \begin{pmatrix} 0 & 0 & 1 \\ 0 & 0 & 0 \\ 1 & 0 & 0 \end{pmatrix}$$

$$\lambda^5 = \begin{pmatrix} 0 & 0 & -i \\ 0 & 0 & 0 \\ i & 0 & 0 \end{pmatrix}$$

$$\lambda^6 = \begin{pmatrix} 0 & 0 & 0 \\ 0 & 0 & 1 \\ 0 & 1 & 0 \end{pmatrix}$$

$$\lambda^7 = \begin{pmatrix} 0 & 0 & 0 \\ 0 & 0 & -i \\ 0 & i & 0 \end{pmatrix}$$

$$\lambda^8 = \frac{1}{\sqrt{3}} \begin{pmatrix} 1 & 0 & 0 \\ 0 & 1 & 0 \\ 0 & 0 & -2 \end{pmatrix}$$

- The non-zero structure constants can be obtained from the commutation relation

$$f^{123} = 1 \qquad f^{147} = -f^{156} = f^{246} = f^{257} = f^{345} = -f^{367} = \frac{1}{2} \qquad f^{458} = f^{678} = \frac{\sqrt{3}}{2}$$

The static quark-antiquark potential

- Computation of the QCD potential can be carried out with Lattice techniques (Wilson loop)

Figure from G. Bali 0001312

